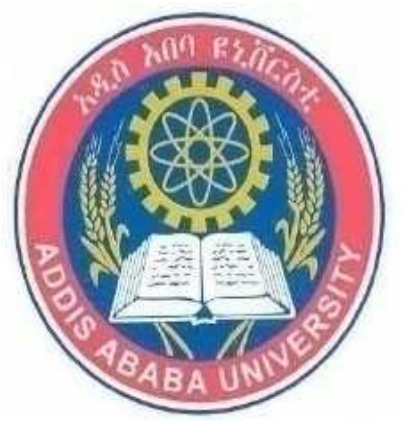

Addis Ababa Institute of Technology (AAiT)

Feasibility Study and Performance Evaluation

(Simulation) of Solar Dryer for Akaki Spare Part and Hand Tools Share Company Moulding Sand Drying Mechanism.

Submitted by

Aschenaki Tadesse

Advisor: Dr.-Ing.Abebayehu Assefa

Addis Ababa, Ethiopia

November 2011

Addis Ababa Institute of Technology

School of Graduate studies

Energy Technology Department

A Thesis Submitted to the School of Graduate Studies of Addis Ababa University in partial Fulfillment of the Degree of Masters of Science in Energy Technology

Submitted by

Aschenaki Tadesse

Advisor: Dr.-Ing.Abebayehu Assefa

Addis Ababa University

Institute of Technology

Department of Energy Center

Graduate Program in Energy Technology

Feasibility Study and Performance Evaluation

(Simulation) of Solar Dryer for Akaki Spare Part and Hand Tools

Share Company Moulding Sand Drying Mechanism

By: Aschenaki Tadesse

Approved by Board of Examiners:-

Chairman, Department of Graduate Committee	Signature	Date
Dr.-Ing Abebayehu Assefa Advisor	Signature	Date
Internal Examiner	Signature	Date
External Examiner	Signature	Date

Acknowledgment

I would like to express may whole hearted deep sense of gratitude to my advisor Dr.-Ing. Abebayehu Assefa and co-adviso Abdurkadir Aman of the Department of Mechanical Engineering for their expert guidance, constructive suggestion and attitude which helps me to submit my thesis work in the present form.

I express my sincere and heartfelt thanks to Mechanical Engineering workshop staff members, particularly, Ato Kassaye who helped me in the construction of some part of solar dryer without any hesitation.

I take this opportunity to acknowledge and thank Akaki Spare Parts and Hand Tools Share Company workers for their help in giving me information and silica sand sample which was used in the experimental investigation of the thesis work.

At last my special thanks go to my beloved brother Endale Tadesse for his everlasting support and his encouragement which helped me to be strong.

Abstract

Silica sand is sand that is used for molding processes. When a catalyst is added to it, it develops the bonding characteristics of the raisin, which binds the silica sand together. Its moisture content (17.24% initial and 0.5% final moisture content) is extremely critical sand additive that can be greatly impact casting quality. In this study flat plate solar collector was used because, it is the most important type of solar collector and it is simple in design, has no moving parts and requires little maintenance. The analysis of heat transfer coefficient (losses) through flat plate collector was discussed and the techniques that used to reduce these losses also mentioned (by using insulation). Mathematical modeling of solar dryer and drying chamber was described. This paper presents designs and performance evaluation of solar dryer for silica sand with its cost estimation. In the dryer, the heated air from a separate solar collector is passed through a tray, and at the same time, vertical blackened wall of the drying chamber, which is exposed to solar radiation. The results obtained during the test period revealed that the temperatures, moisture removed, drying rate and drying efficiency through dying chamber were decreasing during its upraise path. Initial cost of model solar dryer was estimated (2805 ETB). The number of dryer required is eleven so the total cost is equal to 30855ETB.

Table of Content

List of tables

List of figures

Nomenclature

Symbols	Description
T_a	Temperature of Ambient Air, ^{O}C
T_p	Temperature of absorber plate, ^{O}C
T_{ai0}	Temperature of air inlet, ^{O}C
T_g	Temperature of Glass Cover, ^{O}C
T_{ao0}	Temperature of air out let, ^{O}C
T_{sky}	Temperature of sky, ^{O}C
I_N	Solar Intensity, W/m^2
NU	Nusselt number
K	Thermal conductivity of absorber plate
L	Length of absorber plate, m
h_{1c}	Convective heat transfer coefficient from plate to glass, W/m^2
β	Tilt angle
R_a	Rayleigh number
Pr	Prandetell number
h_{2c}	Convective heat transfer coefficient from glass to ambient
G_{rl}	grashof number
V	Wind velocity, m/s
h_{1r}	Radiative heat transfer coefficient from plate to glass cover
h_{2r}	Radiative heat transfer coefficient from glass to ambient
h_1	Total heat transfer coefficient from the plate to cover
h_2	Total heat transfer coefficient from the cover to ambient
U_t	Overall top heat loss coefficient,
U_b	Overall bottom heat loss coefficient
K_{in}	Thermal conductivity of insulation
L_{in}	Insulation thickness
A_C	Collector plate area, m^2
A_e	Collector edge area, m^2
U_e	Edge loss coefficient
U_L	Overall heat loss coefficient

q_u	Useful energy gained by the collector per unit area
Q_u	Useful energy gained by the collector
Q_g	The heat gained by the air
U_{pg}	Overall heat transfer coefficients from the plate to the glass
U_{pab}	Bottom heat transfer coefficient from plate to air
U_{pae}	Edge heat transfer coefficient from plate to air
U_a	Heat transfer coefficient of the air
FR	The collector heat removal factor.
q_L	Overall heat lost by the absorber to the ambient per unit area
$\bar{H}$	Monthly average daily global irradiation [w/m^2]
$\bar{H}_O$	Clear day daily global irradiation [w/m^2]
$\bar{N}_s$	The maximum daily hours of bright sunshine
$\bar{n}_s$	Monthly average daily bright sunshine hours
$\bar{H}_d$	Monthly average daily diffuse radiation [w/m^2]
$\bar{I}$	Monthly average hourly global radiation [w/m^2]
$\bar{I}_d$	Monthly average hourly diffuse radiation [w/m^2]
G_{on}	Extraterrestrial irradiance on a surface at normal incidence [w/m^2]
G_o	Extraterrestrial irradiance incident on a horizontal plane [w/m^2]
H_o	Hourly extraterrestrial irradiance incident on a horizontal plane
δ	Declination angle
ω	Hour angle
τ	Transmittance
α	Solar absorbance
η_c	Overall collector efficiencies
ν	Dynamic viscosity of air.
h_l	The layer drying bed thickness,
ρ	The bulk density of the crop on wet basis
ζ	The sand porosity
ε_v	The loading bed void fraction.
K_a	Thermal conductivity of air.

M_w	Mass of water evaporated from the food item (kg /s).
h_{fg}	Latent heat of vaporization of water (kJ/kg)
M_f	Final moisture content (Kg)
M_i	Initial moisture content (Kg)
η_d	Overall drying efficiencies
m_a	Mass flow rate of air [Kg/s]
$(c_p)_a$	Specific heat of air [J/K]
$(c_p)_p$	Specific heat of plate [J/K]
$(c_p)_g$	Specific heat of glass [J/K]
T_d	Temperature of air out let of first tray, ^{O}C
T_r	Temperature of air out let second tray, ^{O}C
T_{r1}	Temperature of air out let third tray, ^{O}C
$RH:-$	Relative humidity
$M_{cw}:-$	Moisture content wet basis
M_{cd}	Moisture content dry basis
M_d	Dry moisture content
M_w	Wet moisture content
M_c	Moisture content
M_e	Equilibrium moisture content
ε_g	Glass emissivity
ε_p	Plate emissivity
ε_{eff}	Effective emissivity of plate-glazing

CHAPTER ONE

1.1 General Introduction

With the rapid rise in the population and the living standards, the world seems to engulf into major crisis, called energy crisis. If this growth continues with the same speed the condition would go from bad to worse. The reverse of conventional source of energy like coal, petroleum and natural gas are depleting at a very fast rate to fulfill the demand of the growing population. So there is a need to look for some other energy sources that could meet this growing demand. One such source is solar energy, which is cheap available in abundance [7].

Drying is a common technique for preservation of food and other products; including fruits and vegetables. In many rural locations in Africa and most developing countries, grid-connected electricity and supplies of other non-renewable sources of energy are either unavailable, unreliable or, for many farmers, too expensive. Thus, in such areas, crop and other product drying systems that employ motorized fans and/or electrical heating are inappropriate. The large initial and running costs of fossil fuel powered dryers present such barriers that they are rarely adopted by small scale farmers. The traditional open sun drying utilized widely by rural farmers has inherent limitations: high product losses ensure from inadequate drying, fungal attacks, insects, birds and rodents encroachment, unexpected down pour of rain and other weathering effects. In such conditions, solar-energy dryers appear increasingly to be attractive as commercial propositions [16].

Climatic conditions have a great influence on the extent of product losses and deterioration during sun drying. If a climate is warm and dry, product can be held dried. For this to be feasible, the ambient relative humidity during the harvest period must be low enough to ensure that the sample, when dried to its equilibrium moisture content, can be stored safely.

The basic essence of drying is to reduce the moisture content of the product to a level that prevents deterioration within a certain period of time, normally regarded as the ``safe storage period".

Generally Akaki spare part is the largest industry in production of spare parts in Ethiopia. Thus for production of these spare parts it uses casting technology. To produce these spare parts molding sand is primary raw material. Mean while molding sand (silica sand) is washed and dried to improve its quality and efficiency of production. Therefore this thesis (work) focuses on solar energy dryer which is used for drying this washed silica sand to improve the quality and production (efficiency) of the casting technology

Solar energy has been utilized in many applications. Some of its thermal applications are as follows [7]

1. Water heating
2. Space heating
3. Power generation
4. Space cooling and refrigeration
5. Distillation
6. Drying, and
7. Cooking

1.2 General Objective.

The general objective of this thesis is to evaluate the performance of solar dryer and feasibility of the dryer for the molding sand drying mechanism.

1.3 Specific Objective

1. To have higher quality of production
2. To dry the sand at lower drying time
3. To have clean, attractive and pleasant work place.
4. To reduce the number of labors those are involved in drying mechanism (as a result it minimizes the cost).
5. To enhance the competitiveness of the company.
6. To reduce loss (waste) of molding sand by using solar drying technique.
7. To simulate performance of solar dryer by using MATLAB program.
8. To analyze cost of solar dryer.

1.4 Background of the Study

A lot of research work has been carried out throughout the world to investigate and analyze the thermal performance of air heaters. A brief review of literature is presented here [7].

The H.P. Garg, Rakesh Kumar and G.Datta develops a comprehensive simulation model of thermal performance solar tunnel dryer. The basic objective of this paper is to develop a comprehensive simulation model of the thermal performance of solar tunnel dryer. The model is useful in system design as it is sensitive to the design parameters of air collector and dryer (like, length, radius, tunnel tilt, etc.). It is also useful in determining the drying behavior of high-moisture products (vegetables, fruits, etc.) as well as low-moisture products (barely, wheat, etc.). The performance of the dryer has been estimated for a natural convection mode flow. A transient one-dimensional model was developed for the dryer and the numerical calculations were made for the climate of Delhi. It is observed that a large quantity of barley about 2135 kg can be dried in this dryer within two days of operation up to an equilibrium moisture content. (1998 John Wiley & Sons Ltd).

S.Youcef Ali and J.Y. Desmus in 2005 propose Simulation of a new concept of an indirect solar dryer equipped with offset rectangular plate fin absorber-plate. A simulation code was developed to predict the indirect solar dryer performance of the thin beds of discs of potato, subjected to time-varying air conditions. Two mathematical models are developed separately; the first allows the determination of the thermal performances of the solar collector with offset rectangular plate fin absorber-plate and the second, allows to determine the kinetics of drying for the data input of the air at the exit of the collector. The latter takes into account calorific losses through the walls of the dryer and shrinkage of discs. Experimental results of the solar dryer thermal performances, using sunlight in Valenciennes (in the North of France), was compared with the results obtained by the theoretical model suggested.

P. A. Potdukhe and S. B. Thombre In 2008 studied the Development of a new type of solar dryer: Its mathematical modeling and experimental evaluation. Under their investigation they observe the drying period as well as the quality of dried products. Thermic oil was used as a storage material. The main objective of the study was to reduce the drying period and enhance the quality of dried product mainly chillies and fenugreek leaves. The products were laid in a single layer. The mass of thermic oil needed in the absorber and mass of product to be dried in trays were optimized using simulation techniques. The maximum drying air temperature required for drying agricultural products was around 65 ^{o}C: The ambient conditions at the location were 25–40 ^{o}C; 16–43% RH and solar radiation 105–1024W/m^{2}: Experimental studies based on temperature

and humidity measurements were performed on the dryer. The research concluded that the desired drying air temperature was achieved and maintained for a longer period. The length of operation of the solar air heater and the efficiency of the dryer were increased, and better quality of agricultural products in terms of colour value was obtained compared with open sun drying.

Abdullah Akbulut and Aydin Durmus in 2009 propose thin layer solar drying and mathematical modeling of mulberry. In this study, drying parameters of mulberry grown in Elazing were investigated as experimental and theoretical using solar dryer system. The drying experiments were conducted at seven different drying mass flow rates varied between

0.0015 and 0.036 kgs^{-1}. As results of the drying experiments were conducted at different drying mass flow rates, it was shown that the drying time was decreased with the drying mass flow rate. This paper also presents a new mathematical modeling of thin layer solar drying of mulberry samples.

Bolaji Bukola .O and. Olalusi Ayoola proposes Performance Evaluation of a Mixed-Mode Solar Dryer; Abeokuta, Ogun State, Nigeria; 2008. This paper presents the design, construction and performance evaluation of a mixed-mode solar dryer for food preservation. In the dryer, the heated air from a separate solar collector is passed through a grain bed, and at the same time, the drying cabinet absorbs solar energy directly through the transparent walls and roof. The results obtained during the test period revealed that the temperatures inside the dryer and solar collector were much higher than the ambient temperature during most hours of the day-light. The temperature rise inside the drying cabinet was up to 74% for about three hours immediately after 12.00h (noon). The drying rate and system efficiency were 0.62 kg/h and 57.5% respectively. The rapid rate of drying in the dryer reveals its ability to dry food items reasonably rapidly to a safe moisture level.

Assefi Hossein and Atikol. U discussed on Performance Potential of Flat Plate Solar Air Heaters in Tehran [2009]. In this paper the results of a parametric study on using solar air heaters in Tehran is presented. Simulations were performed for a typical small building by writing a computer program in FORTRAN. It is found that as the mass flow rate of air decreases the outlet temperature increases in the expense of decreasing efficiency. On the other hand, as the air channel depth is changed between 12 mm and 24 mm the useful energy gain is almost unaltered. Moreover, the simulation program is extended to evaluate the performance of solar air heaters on a typical winter day under the climatic condition of Tehran, where solar heating collectors are barely used.

Rajkumar Perumal [2007] proposed Comparative Performance of Solar Cabinet, Vacuum Assisted Solar and Open Sun Drying Methods. The sun drying has been used for

the preservation, it is a slow process and the quality of the dried product is often inferior due to contaminations. Therefore, a lab model solar cabinet and vacuum assisted solar dryers were developed to study the drying kinetics of tomato slices (4, 6 and 8 mm thicknesses) and the results were compared individually with open sun drying under the weather conditions of Montreal, Canada. The drying kinetics using thin layer drying models and the influence of weather parameters such as ambient air temperature, relative humidity, solar insulations and wind velocity on drying of tomato slices were evaluated.

Forson.F.K.Nazha, M.A.A.Akuffo F.O. and Rajakaruna.H (2007). A mixed-mode natural convection solar crop dryer (MNCSCD) designed and used for drying cassava and other crops in an enclosed structure is presented. A prototype of the dryer was constructed to specification and used in experimental drying tests. This paper outlines the systematic combination of the application of basic design concepts, and rule of thumb resulting from numerous and several years of experimental studies used and presents the results of calculations of the design parameters. A batch of cassava 160 kg by mass, having an initial moisture content of 67% wet basis from which 100 kg of water is required to be removed to have it dried to a desired moisture content of 17% wet basis, is used as the drying load in designing the dryer. A drying time of 30–36 h is assumed for the anticipated test location (Kumasi; 6.71N, 1.61W) with an expected average solar irradiance of 400W/m2 and ambient conditions of 25 1C and 77.8% relative humidity. A minimum of 42.4m^2 of solar collection area, according to the design, is required for an expected drying efficiency of 12.5%.

CHAPTER TWO

Literature Review

2.1 Solar Dryer Theory

Solar dryers have the principal advantage of using solar energy a free, available, and limitless energy source that is also non-polluting. Solar dryers use the energy of the sun to heat the air that flows over the product in the dryer. As air is heated, its relative humidity decreases and it is able to hold more moisture. Warm, dry air flowing through the dryer carries away the moisture that evaporates from the surfaces of the product.

2.2 Drying Mechanism

Drying involves the extraction of moisture from the product by heating and the passage of air mass around it to carry away the released vapor. Under ambient conditions, these processes continue until the vapor pressure of the moisture held in the product equals that held in the atmosphere. Thus, the rates of moisture desorption from the product to the environment and absorption from the environment is in equilibrium, and the sample moisture content at this condition is known as the equilibrium moisture content. Under ambient conditions, the drying process is slow, and in environments of high relative humidity, the equilibrium moisture content is insufficiently low for safe storage .The objective of a dryer is to supply the product with more heat than is available under ambient conditions, thereby increasing sufficiently the vapor pressure of the moisture held within the product and decreasing significantly the relative humidity of the drying air and thereby increasing its moisture carrying capacity and ensuring a sufficiently low equilibrium moisture content .

Drying preserves silica sand by removing enough moisture from silica sand to prevent casting defect and increase quality of manufacturing products by removing the moisture to safe level.

Solar dryer is working on the principle that hot air absorbs more moisture than cooled air. Air is heated by specially designed solar collectors and passed through a chamber for drying.

2.3 Classification of Solar Dryers

All drying systems can be classified primarily according to their operating temperature ranges into two main groups of high temperature dryers and low temperature dryers. However, dryers are more commonly classified broadly according to their heating sources into fossil fuel dryers (more commonly known as conventional dryers) and solar-energy dryers. Strictly, all practically-realized designs of high temperature dryers are fossil fuel

powered, while the low temperature dryers are either fossil fuel or solar-energy based systems.

2.3.1 High Temperature Dryers

High temperature dryers are necessary when very fast drying is desired. They are usually employed when the products require a short exposure to the drying air. Their operating temperatures are such that, if the drying air remains in contact with the product until equilibrium moisture content is reached, serious over drying will occur.

2.3.2 Low Temperature Dryers

In low temperature drying systems, the moisture content of the product is usually brought in equilibrium with the drying air by constant ventilation. Thus, they do tolerate intermittent or variable heat input. Low temperature drying enables products to be dried in bulk and is most suited also for long term storage systems. Their ability to accommodate intermittent heat input makes low temperature drying most appropriate for solar-energy applications. Thus, some conventional dryers and most practically-realized designs of solar-energy dryers are of the low temperature type.

2.4 Classification of Solar-Energy Drying Systems

Solar-energy drying systems are classified primarily according to their heating modes and the manner in which the solar heat is utilized.

In broad terms, they can be classified into two major groups,

2.4.1 Active Solar-Energy Drying Systems

Active solar drying systems depend only partly on solar-energy. They employ solar-energy and/or electrical or fossil-fuel based heating systems and motorized fans and/or pumps for air circulation. All active solar dryers are, thus, by their application, forced-convection dryers. Major applications of active solar dryers are in large-scale commercial drying operations in which air heating solar-energy collectors supplement conventional fossil-fuel fired dehydrators, thus reducing the overall conventional energy consumption, while maintaining control of the drying conditions. If warm enough, the solar-heated air could be used directly for the drying process; otherwise the fossil-fuel fired dehydrator would be used to raise the drying air temperature to the required level, thus avoiding the effects of fluctuating energy output from the solar collector, since the fossil-fuel system can be controlled automatically to provide the required optimum drying conditions. These active solar dryer types that incorporate dehydrators for supplemental heating are commonly known as ``hybrid solar dryers'' [15 16].

Three distinct sub-classes of active are:-

1. Integral-type (direct) solar dryers
2. Distributed-type (indirect) solar dryers
3. Mixed-mode solar dryers

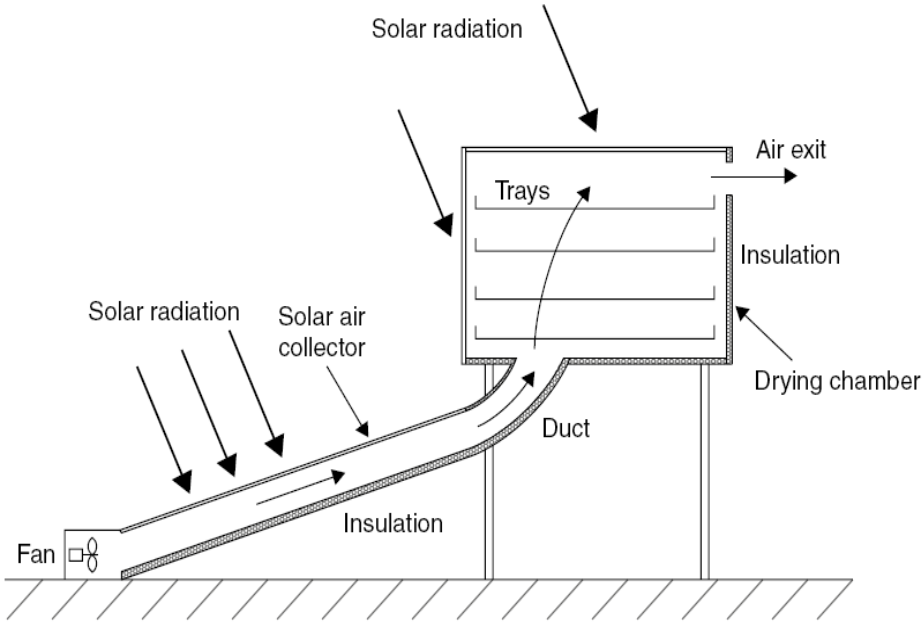

Figure 2.1 Schematic Diagram of a Forced Circulation, Mixed-Mode Solar Energy Dryer

2.4.2 Passive Solar Drying Systems

Natural-circulation solar-energy dryers depend for their operation entirely on solar-energy.

In such systems, solar-heated air is circulated through the sample to be dried by buoyancy forces or as a result of wind pressure, acting either singly or in combination. These dryers are often called passive. Similarly like active solar drying system there are three distinct sub-classes of passive solar drying systems which can be identified mainly in their design arrangement of system components and the mode of utilization of the solar heat, namely [15 16].

1 Integral-Type (direct) Solar Dryers

In integral-type natural-circulation solar-energy dryers (often termed direct solar dryers), the product is placed in a drying chamber with transparent walls that allow the insulation necessary for the drying process to be transmitted. Thus, solar radiation impinges directly on the product. The heat extracts the moisture from the product and concomitantly (alongside) lowers the relative humidity of the resident air, thereby increasing its moisture

carrying capability. In addition, it expands the air in the chamber, generating its circulation and the subsequent removal of moisture along with the warm air.

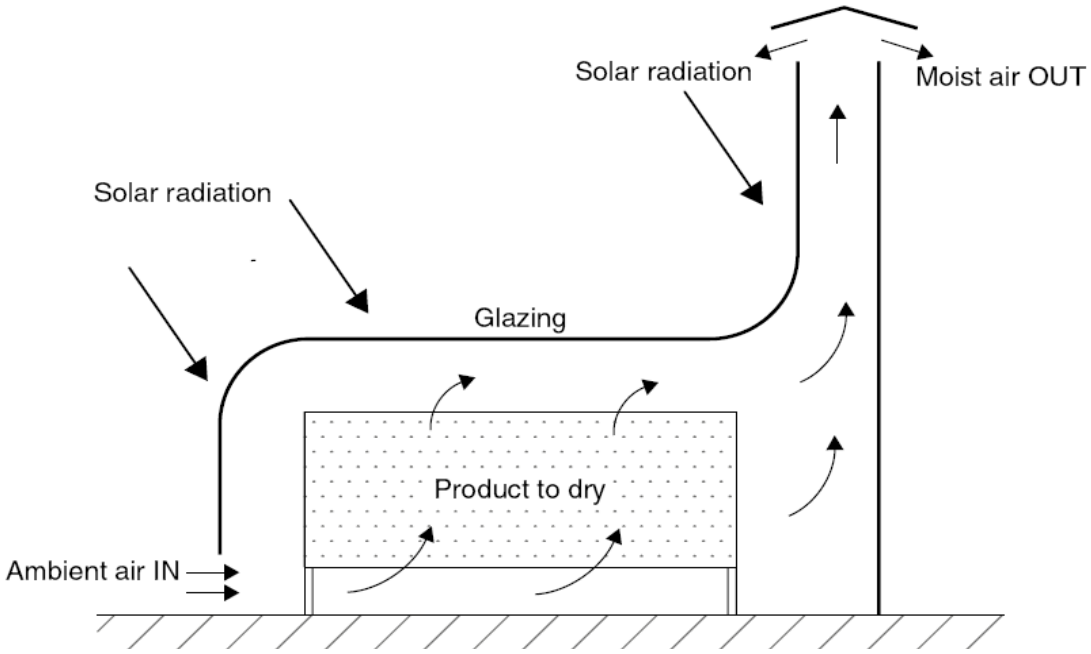

Figure 2.2 Schematic Diagram of a Natural Circulation, Direct-Mode Solar Energy Dryer

2 Distributed-Type (indirect) Solar Dryers

These are often termed indirect passive solar dryers. Here, the sample is located in trays or shelves inside an opaque drying chamber and heated by circulating air, warmed during its flow through a low pressure drop thermos phonic solar collector. Because solar radiation is not incident directly on the silica sand, it is not over heated.

A typical distributed natural-circulation solar-energy dryer would be comprised of the following basic units:

1. An air-heating solar-energy collector;
2. Appropriate insulator;
3. A drying chamber; and
4. A chimney**.**

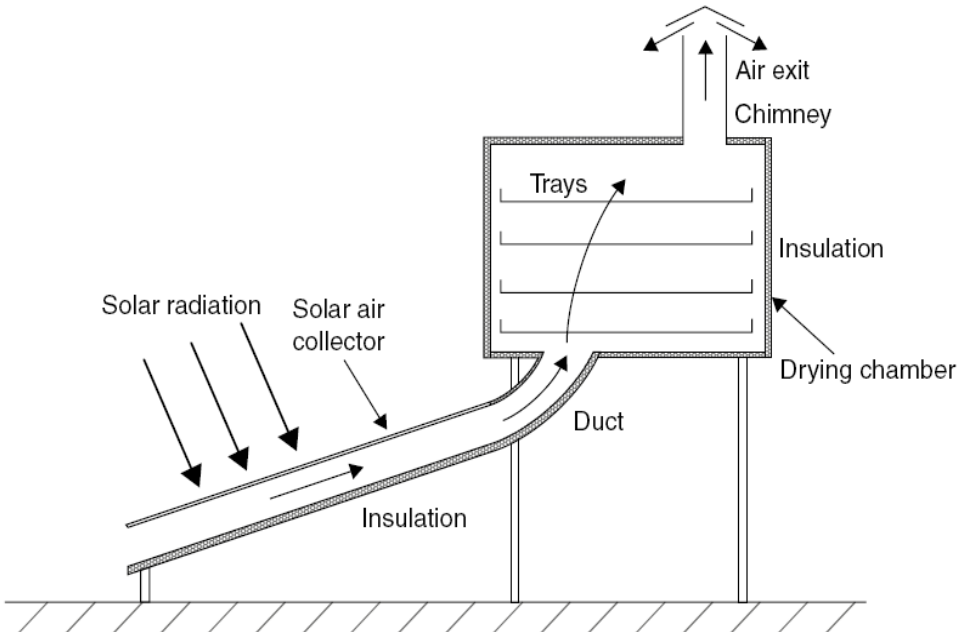

Figure 2.3 Schematic Diagram of a Natural Circulation, Indirect-Mode Solar Energy Dryer

3 Mixed-Mode Solar Dryers

These dryers combine the features of the integral (direct) type and the distributed (indirect) type natural-circulation solar-energy dryers. Here the combined action of solar radiation incident directly on the product to be dried and pre-heated in a solar air heater furnishes the necessary heat required for the drying process. A typical mixed-mode natural- circulation solar-energy dryer would have the same structural features as the distributed-type (i.e. a solar air heater, a separate drying chamber and a chimney), but in addition, the walls of the drying chamber are glazed so that the solar radiation impinges directly on the product as in the integral-type dryers**.**

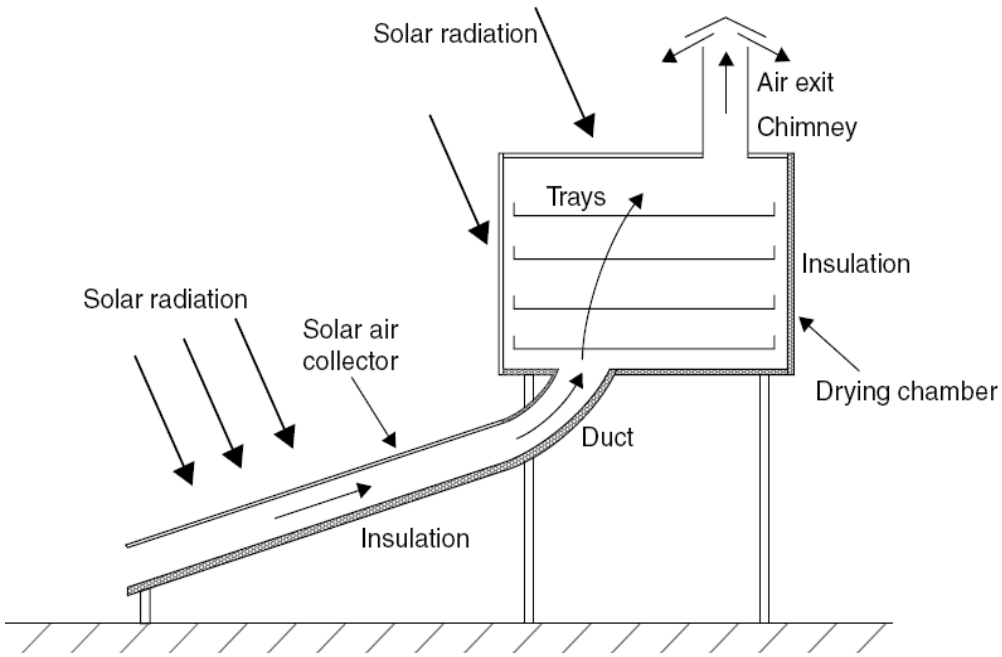

Figure 2.4 Schematic Diagram of a Natural Circulation, Mixed-Mode Solar Energy Dryer

2.5 Introduction to Solar Collectors

In any solar-thermal collection device, the principle usually followed is to expose a dark surface to solar radiation so that most of the solar radiation is absorbed and converted heat energy. A part of this heat energy is then transferred to a fluid like water or air. When no optical concentration of radiation is done, the device in which the collection is achieved is called the flat plate collector. In other words, when the area of interception of solar radiation is same as that of absorption then the collection device is called flat-plate collector else it is concentrating collector. The flat plate collector is the most important type of solar collector because it is simple in design, has no moving parts and requires little maintenance. It can be used for variety of applications in which temperature of required heat energy ranges from 40-100 ^{0}C [7].

2.5.1 Concentrating Collector

Concentrating collectors use mirrored surfaces to concentrate the sun's energy on an absorber called a receiver as shown in figure below. Concentrating collectors also achieve high temperatures, but unlike evacuated-tube collectors, they can do so only when direct sunlight is available. The mirrored surface focuses sunlight collected over a large area onto a smaller absorber area to achieve high temperatures. Some designs concentrate solar energy onto a focal point, while others concentrate the sun's rays along a thin line called the focal line. The receiver is located at the focal point or along the focal line. A heat-transfer fluid flows through the receiver and absorbs heat. These collectors reach much higher temperatures than flat-plate collectors. However, concentrators can only focus

direct solar radiation, with the result being that their performance is poor on hazy or cloudy days.

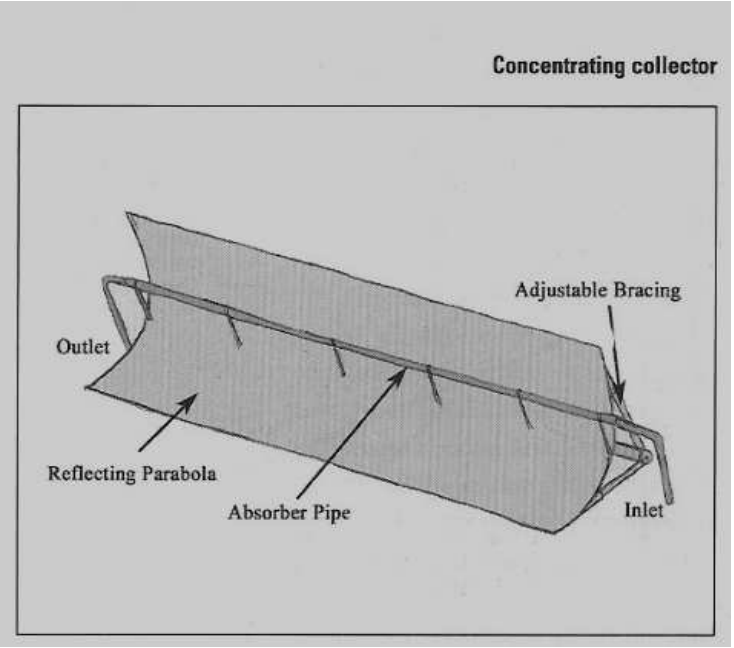

Figure 2.5 Schematic Representation of Concentrating Collector

There are four basic types of concentrating collectors:

1. Parabolic trough
2. Parabolic dish
3. Power tower
4. Stationary concentrating collectors

2.5.2 Flat-Plate Collectors

Flat-plate collectors are very common and are available as liquid based and air-based collectors. These collectors are better suited for moderate temperature applications where the demand temperature is 30-70 ^{0}C and/or for applications that require heat during the winter months.

The air-based collectors are used for the heating of buildings, ventilation air, and for drying crop and industry products. In this type of collector a flat absorber plate efficiently transforms sunlight into heat. To minimize heat escaping, the plate is located between a glazing (glass pane or transparent material) and an insulating panel. The glazing is chosen so that a maximum amount of sunlight will pass though it and reach the absorber. Figure below represents the constructional features of flat plate collectors.

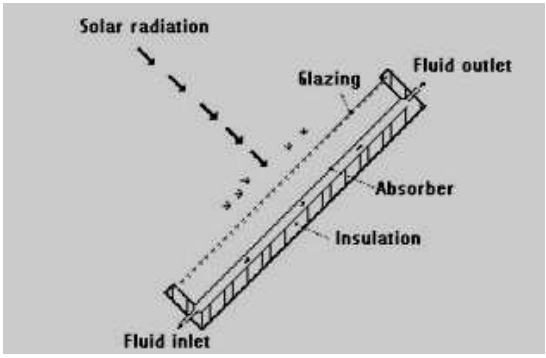

Figure 2.6 Represents the Constructional Features of Flat Plate Collectors.

2.5.3 Optimization of Collector

Apart from the effect of characteristics of the collector itself, the output of solar collector strongly depend on the inclination angle of solar collector. [16]

Table 2.1 Orientation of Tilt Angle for Selected Months.

Latitud	Best collector tilt in:					
e	June (degree)	Orientation	Sept./march(degree)	Orientation	December (degree)	Orientation
50	26.5	S	50	S	73.5	S
40	16.5	S	40	S	63.5	S
30	6.5	S	30	S	53.5	S
20	3.5	N	20	S	43.5	S
15	8.5	N	15	S	38.5	S
10	13.5	N	10	S	33.5	S
Equator =0	23.5	N	Equator =0	-	23.5	S
10	33.5	N	10	N	13.5	S
15	38.6	N	15	N	8.5	S
20	43.5	N	20	N	3.5	S
30	53.5	N	30	N	6.5	N
40	63.5	N	40	N	16.5	N
50	73.5	N	50	N	26.5	N

The largest yield is obtained when the collector is always oriented perpendicular to the sun. However, the optimal tilt angle for the collector varies according to the season, as the sun is higher in the sky in summer than in winter. As a general rule the optimal angle of tilt is equal to the degree of latitude of the site. But the minimum angle of the collector should be 15 degree to assist the thermo siphon effect [16].

2.6 Application Flat Plate Collector

2.6.1 Solar Water Heater

In Solar water heater, water is heated by the use of solar energy. Solar heating systems are generally composed of solar thermal collectors, a fluid system to move the heat from the collector to its point of usage. The system may use electricity for pumping the fluid, and have a reservoir or tank for heat storage and subsequent use. The systems may be used to heat water for a wide variety of uses, including home, business and industrial uses. Heating swimming pools, under floor heating or energy input for space heating or cooling are more specific examples

2.6.2 Solar Air Heater

A solar air heater is a simple device to heat air by utilizing solar energy, which has many applications in drying agricultural products, such as seeds, fruits and vegetables, industrial products and as a low-temperature energy source. Also, solar air heaters are utilized for heating buildings with auxiliary heaters to save energy in winter-time. Solar air heaters can also be used for industrial purposes. Radiation energy of sun is absorbed by an absorber plate and then transferred to air. This heated air can be used further according to our requirement. Different configurations are possible for air flow in the passage. Solar air heaters are simple in design and maintenance.

2.7 Heat Transfer Analysis for Flat Plate Collector

2.7.1 Heat Loss Coefficient of Flat Plate Collector

It is useful to develop the concept of an overall loss coefficient for a solar collector to simplify the mathematics. Consider the thermal network for one-cover system shown below.

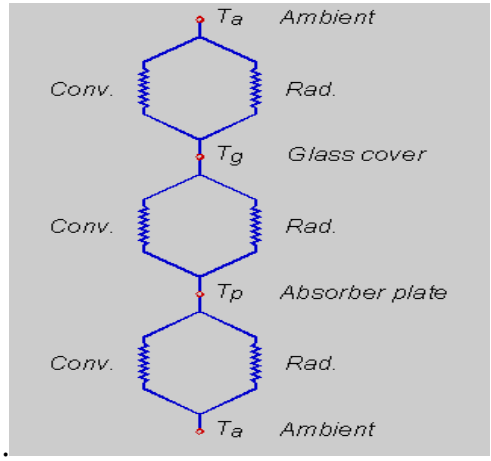

Figure 2.7 Thermal Network for One-Cover System

Heat is lost to the surroundings from the plate through:

The glass cover (referred as top loss), and the insulation (referred as bottom and edge loss) [1].

I. Top Loss Coefficient

The top loss coefficient of flat plate collector is analyzed by considering three different heat transfer methods as follows.

A. Convective Heat Transfer Coefficient

a) From Plate to Glass Cover

$$h_{1c} = NU\frac{K}{L} \tag{2.1}$$

Nu the Nusselt number-the ratio of the convective heat transfer to the conductive heat transfer.

The Nu can be obtained from the expression (Holland et. al. (1976)) [1].

$$NU = 1 + 1.44\left[1 - \frac{1708}{Ra * \cos\beta}\right]^{+} * \left[1 - \frac{1708\sin(1.8\beta)^{1.6}}{Ra * \cos\beta}\right] + \left[\left(\frac{Ra * \cos\beta}{5830}\right)^{1/3} - 1\right]^{+} \tag{2.2}$$

"+" exponent means only the positive value of the term in square bracket is to be considered. Zero is to be used for negative values.

The Rayleigh number Ra is given by:

$$R_a = Grl * \Pr = \frac{g\beta\Delta t L^3}{v^2}\Pr \tag{2.3}$$

b) From Glass Cover to Ambient

$$h_{2c} = 2.8 + 3 * V \tag{2.4}$$

Where: V is the wind velocity in m/s, over the collector

B. Radiative Heat Transfer Coefficient

a) From Plate to Cover

h_{lr} is the coefficient of radiative heat loss from collector plate to the cover, expressed as:

$$h_{1r} = \varepsilon_{eff}\sigma\left[\frac{(T_p + 273)^4 - (T_g + 273)^4}{T_p - T_g}\right] \tag{2.5}$$

The effective emissivity of plate-glazing system is given by:

$$\varepsilon_{eff} = \frac{1}{\frac{1}{\varepsilon_p} + \frac{1}{\varepsilon_g} - 1} \tag{2.6}$$

b) From Glazing Cover to Ambient.

The sky temperature T_{sky} given by:

$$T_{sky} = T_a - 6 \tag{2.7}$$

The radiative heat transfer coefficient is expressed as:

$$h_{2r} = \varepsilon_g\sigma\left[\frac{(T_g + 273)^4 - (T_{sky} + 273)^4}{T_g - T_a}\right] \tag{2.8}$$

The total heat transfer coefficient from collector plate to cover is expressed as the sum of h1c and h1r.

$$h_1 = h_{1c} + h_{1r} \tag{2.9}$$

The total heat transfer coefficient from the cover to ambient is expressed as:

$$h_2 = h_{2c} + h_{2r} \tag{2.10}$$

The effective top heat transfer coefficient from plate to ambient is given by:

$$U_t = \frac{1}{\frac{1}{h_1} + \frac{1}{h_2}} \tag{2.11}$$

Finally the rate of heat loss from the top per unit area can be given as:

$$q_{losstop} = U_t (T_p - T_a) \tag{2.12}$$

II. Back Loss Coefficient

Heat is lost from the plate to ambient by conduction through the insulation and subsequently by convection and radiation from the bottom surface casing.

The bottom loss coefficient is given by:

$$U_b = \frac{1}{\frac{L_{in}}{K_{in}} + \frac{1}{h_b}} \tag{2.13}$$

The magnitude of $\frac{L_{in}}{K_{in}}$ and $\frac{1}{h_b}$ are such that the second term in the Equation (2.13) is negligible. Therefore

$$U_b = \frac{K_{in}}{L_{in}} \tag{2.14}$$

III. Edge Loss Coefficient

Energy lost from the side of the collector casing may be taken to have exactly the same value as that from the back, if the thickness of the edge insulation is the same as that of the back insulation (Tabor, 1958). The edge loss is given as:

$$U_e = U_b \left[\frac{A_e}{A_c} \right] \tag{2.15}$$

IV. Overall Heat Loss Coefficient

The overall heat loss coefficient U_L is the sum of the top, bottom and edge loss coefficient. That is:

$$U_L = U_t + U_b + U_e \tag{2.16}$$

The overall heat lost by the absorber to the ambient per unit area per unit time can be expressed as:

$$q_L = U_L\left(T_p - T_a\right) \tag{2.17}$$

The useful energy gained by the collector is expressed as:

$$Q_u = \alpha\tau INA_c - A_c U_L\left(T_{p0} - T_{ai0}\right) \tag{2.18}$$

Therefore, the energy per unit area (qu) of the collector is:

$$Q_u = \alpha\tau IN - U_L\left(T_{p0} - T_{ai0}\right) \tag{2.19}$$

If the heated air leaving the collector is at collector temperature, the heat gained by the air Qg is:

$$Q_g = \dot{m} * cpa\left(T_{p0} - T_{ai0}\right) \tag{2.20}$$

The collector heat removal factor, FR, is the quantity that relates the actual useful energy gained of a collector, to the useful gained by the air, Therefore,

$$FR = \frac{\dot{m} * cpa\left(T_{p0} - T_{ai0}\right)}{\alpha\tau INA_c - A_c U_L\left(T_{p0} - T_{ai0}\right)} \tag{2.21}$$

Or

$$Q_g = A_c * FR\left(\sigma\tau IN - U_L\left(T_{p0} - T_{ai0}\right)\right) \tag{2.22}$$

The thermal efficiency of the collector is defined as:

$$\eta_c = \frac{Q_g}{A_c * I_N} \tag{2.23}$$

2.8 Introduction to Solar Radiation

In spite of abundant availability of solar energy in the tropics the determination of the quantity of energy available at any location has posed various challenges [19]. This is because the quantity of solar energy available within these regions are dependent on the latitude, hour of the day, day of the year, altitude, and clearness of the sky and these values need to be determined and evaluated for the solar radiation incident at a location itself. In addition, the amount of global solar insulation at a place could be established by measurements, which is a tedious process, and many consumers of such information lack the tools to carry out physical measurements (especially in developing country such as Ethiopia). Besides, the common practice has been to develop models which can predict the energy incident at a particular location at any time. Such energy can then be used as an input variable in the design of solar energy application systems such as solar air and water heaters, and solar dryers among other uses.

2.8.1 Solar Energy Measurement

The annual, monthly, daily and hourly records of the amount of solar radiation received at any given location over the earth's surface are essential for the design of solar energy systems. Therefore, solar radiation measurements are made continuously at monitoring stations of country [1].

Measurements may include, direct component at normal incidence, diffuse component at a horizontal surface, global radiation on a horizontal surface, total radiation on an inclined surface, ground reflected radiation, and spectral distribution over certain wavelength bands.

A variety of instruments are used for the measurement of solar radiation. They are categorized into two groups: pyranometers and pyrheliometers. Pyranometers are used to measure the total radiation, incident on a horizontal surface from the entire sky. They can also measure the diffuse component if covered by an appropriate shade band. Operation of most pyranometers is based on measurement of temperature difference between black and white elements using a thermopile.

Pyrheliometers measure the intensity of the direct solar radiation at normal incidence. Most pyrheliometers used for routine (practice) measurements operate on the thermopile effect so are similar to pyranometers in this respect. They differ in that mechanically they must follow the sun to measure the direct sunlight only and avoid the diffuse component. In practice, direct solar radiation is measured by attaching the instrument to an electrically driven equatorial mount for tracking the sun.

Apart from the direct solar radiation records, there may be records of bright sunshine hours and approximate cloud cover for the location under interest. Sunshine recorders are

devices that measure hours of bright sunshine, not energy. These devices are sensitive only to the direct component of solar radiation when it is above some imprecise threshold. The Campbell sunshine recorder is the classic recorder widely used throughout the world.

Empirical formulas are required for estimation of radiation, for locations at which insufficient or no measurements are available. Various climatological parameters such as humidity, temperature, rainfall, number of sunshine hours and total amount of cloud coverage have been used in developing empirical relations as substitutes for the direct measurement.

Three basic problems can be clearly identified as most relevant when estimation of radiation components arriving on a collector surface:

1. Evaluation of the global radiation from other meteorological variables such as percent sunshine hours, extent of cloud cover, relative humidity, etc.

2. Conversion of daily radiation components into hourly values.

3. Conversion of the horizontal components of the radiation into equivalent inclined components.

Radiation data on hourly basis may be estimated from daily records although such computation may not be accurate and may even be completely misleading. The reason is that different combinations of cloudy periods and sunny hours may result in the same daily total radiation**.** The hourly solar radiation on a horizontal surface is found to be dependent on the sunset hour angle.

2.9 Solar Radiation for Addis Ababa

The performance of solar dryer is significantly depends on the weather condition of the location (Addis Ababa) which means the heat required to remove the moisture from the product to be dried is only from solar energy. So the weather conditions have a biggest influence on the capacity of product that can be dried with certain time period.

Since measurements of radiation components requires expensive equipment that is costly to operate as well as maintain, reliable measurements are undertaken at only a limited number of stations. Thus the Ethiopian Meteorological Service collects solar radiation data for some cities of the country. Hence in Addis Ababa this solar radiation data can be used as an input variable in the design of solar dryers for molding sand of Akaki Spare Part and Hand Tools Share Company.

2.9.1 Extraterrestrial Irradiance

The extraterrestrial irradiance on a surface at normal incidence (G_{on}) may be expressed as

$$G_{on} = G_{sc}\left[1 + 0.033\cos\left(\frac{2\pi n}{365}\right)\right] \tag{2.28}$$

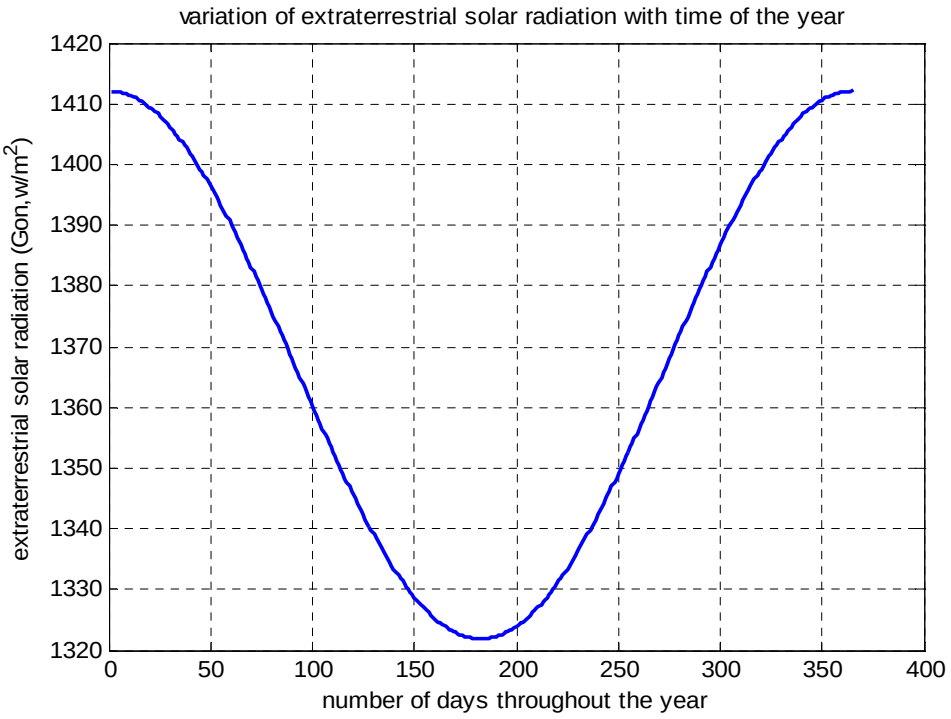

Figure 2.8 Variation of Extraterrestrial Solar Radiation with Time of the Year

Where n is the number of the day in the year with January 1st representing a value of 1 and December 31 a value of 365.

The extraterrestrial irradiance incident on a horizontal plane at an arbitrary angle of incidence is also of interest and is given by,

$$G_o = I_N\left(1 + 0.033\cos\frac{360n}{365}\right) * \left(\cos\phi\cos\delta\cos\omega + \sin\phi\sin\delta\right) \tag{2.29}$$

When it is given hourly

$$H_o = \frac{24 * 3600 I_N}{\pi}\left(1 + 0.033\cos\frac{360n}{365}\right) * \left(\cos\phi\cos\delta\cos\omega + \sin\phi\sin\delta\right) \tag{2.30}$$

2.9.2 Declination Angle

The time of the year is represented by the solar declination angleδ, which is defined as the angle between the earth's equatorial plane and the earth sun line.

Because of the earth's elliptic orbit around the sun and the variation in the sun-earth distance, the solar declination angle varies from positive 23.45^0 north equator on the 21st June to negative 23.45^0 south of equator on the 21st December. It is customarily approximated by,

$$\delta = 23.45 \sin\left(2\pi \frac{284+n}{365}\right) \tag{2.31}$$

Where n is the number of the day in the year.

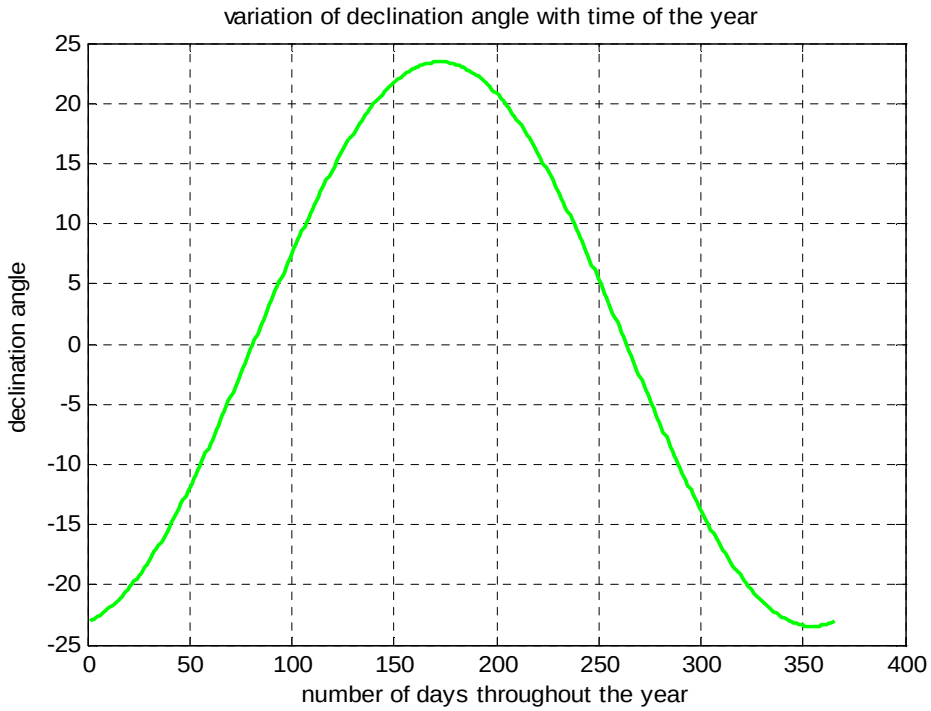

Figure 2.9 Variation of Declination Angle with Time of the Year.

2.9.3 Hour Angle

The time of the day is expressed in terms of the hour angleω. It is taken to be zero at local solar noon, increases by 15^0 for each hour before local solar noon and decreases at the same rate after solar noon.

$$\omega = (ST - 12) * 15^o \tag{2.32}$$

Where: - ST is the local solar time in hours

Solar radiation data was simulated for respective days at which the experiment was conducted. This data was obtained from Addis Ababa (Bole) Metrology which is the nearest location for the site.

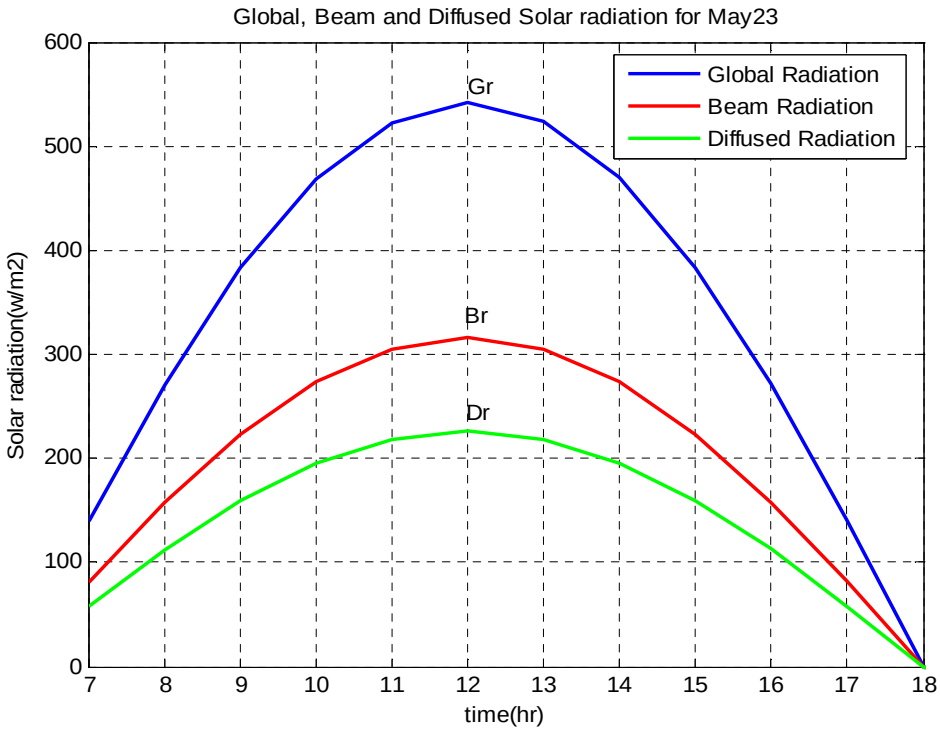

Figure 2.10 Global, Beam and Diffused Solar radiation for May 23

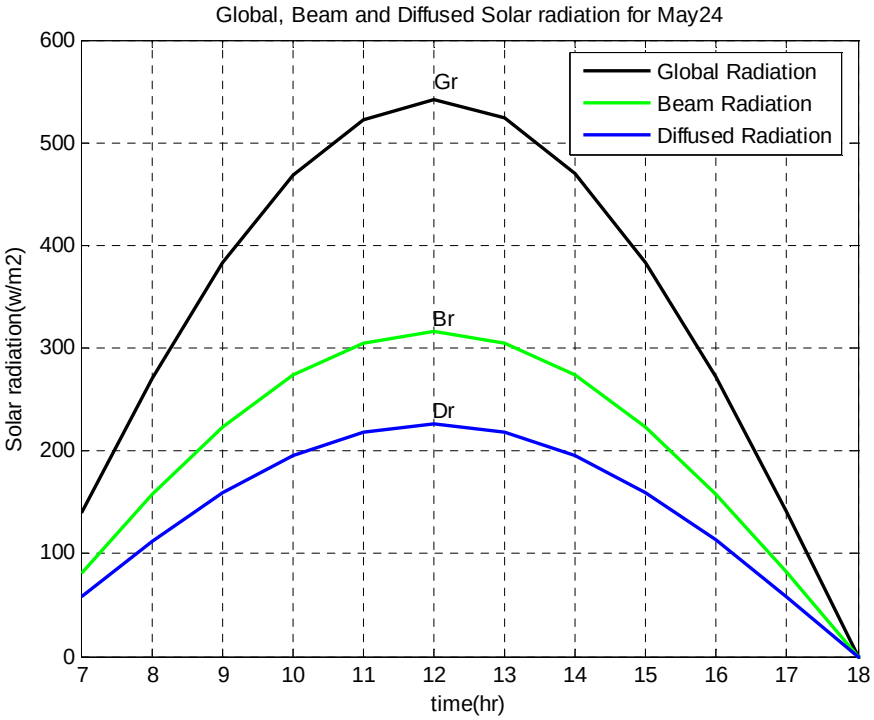

Figure 2.11 Global, Beam and Diffused Solar radiation for May 24

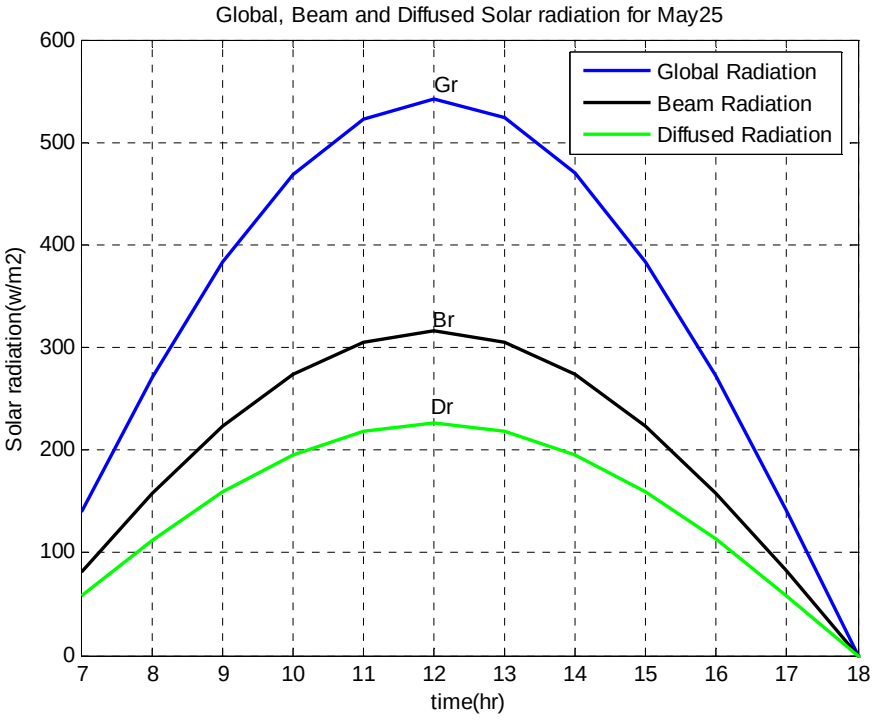

Figure 2.12 Global, Beam and Diffused Solar radiation for May 25

CHAPTER THREE

Molding sand

3.1 Introduction

The Sand Casting molding process utilizes a cope (top half) and drag (bottom half) flask set-up. The mold consists of sand, (usually silica), raisin and catalyst. When the catalyst is added it develops the bonding characteristics of the raisin, which binds the silica sand together. When applying pressure to the mold material it can be compacted around a pattern, which is either made of metal or wood, to produce a mold having sufficient rigidity to enable metal to be poured into it to produce a casting. The process also uses coring to create cavities inside the casting. After the casting is poured and has cooled the core is removed.

The material costs for the process are low and the sand casting process is exceptionally flexible. A number of metals can be used for castings in sizes from ounces to many thousand pounds. The mold material is reclaimable, with between 90 and 95% of the sand being recycled, although new sand and additions are required to make up for the discarded loss. These features, combined with the relative ease of mold production, have ensured that the silica sand molding process has remained as the principal method by which castings are produced.

3.2 Sand

The size and distribution of sand grain are extremely important in controlling the surface finish of the casting. The characteristic also affect the ability of the mold to promote the evacuation of gases formed during the transformation of water to steam and the decomposition organic constitute of the core binders and silica sand additives. The correct sand distribution is also critical in reducing the occurrence of sand expansion defect.

Figure 3.1 washed silica sand

3.3 Patterns

Making a pattern is similar to making the piece in wood, with some differences of course. The first difference is that the pattern must be made bigger than the final piece. When the metal melts it expands, and it will contract after being poured into the mold.

Another difference is that any vertical surface, as viewed when the pattern is in the mold, must be tapered. The taper is required to make it easier to remove the pattern from the mold.

3.4 Making mold

The mold is made in a box called a flask. A flask is made with two or more interconnecting parts. Figure below shows a two-part flask. The following figure shows that piece on the left is the bottom and it is called the drag. The piece on the right is the top, and it is called the cope. When the parts are put together the pegs in the cope will fit into the sockets on the drag. This assured the flask goes together the same way each time. The edges of the cope and drag shown in the picture are where the parting line of the mold will be.

Figure 3.2 cop and drag of molding sand

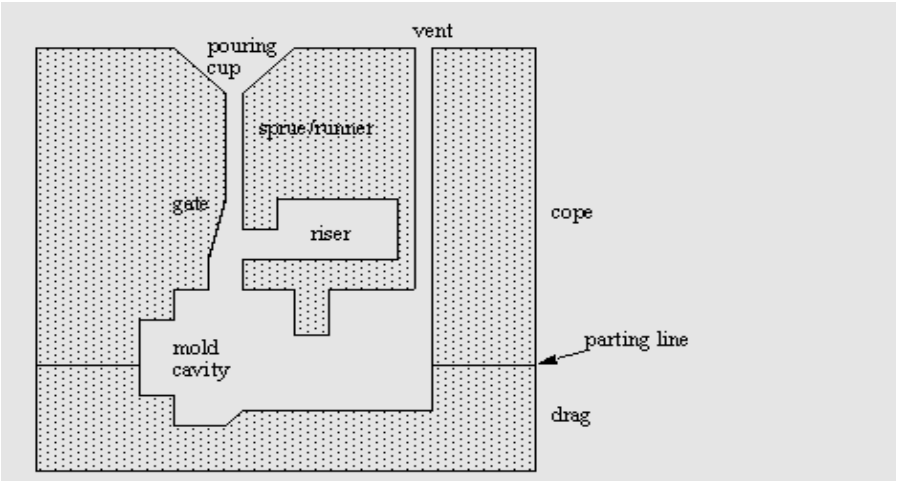

Figure 3.3 schematic diagram of making mold.

Terms that are shown in the above figure are described as follows.

1. Pouring cup: This is where the metal is poured into the mold.
2. Sprue: The vertical channel from the top of the mold to the gating and riser system. Also, a generic term used to cover all gates, runners and risers.
3. Runner: The portion of the gate assembly that connects the sprue to the casting in gate or riser.
4. Gate: The end of the runner in a mold where molten metal enters the mold cavity.
5. Riser: A reservoir of molten metal provided to compensate for the contraction of the metal as it solidifies.
6. Mold cavity: The impression in a mold produced by the removal of the pattern. When filled with molten metal it forms a casting.
7. Cope: Upper or top most section of a flask, mold or pattern.
8. Parting line: A line on a pattern or casting corresponding to the separation between the parts of a mold.
9. Drag: Lower or bottom section of a flask, mold or pattern

3.5 Moisture Measurement of Silica Sand in Foundry.

Moisture is extremely critical sand additive that can be highly affect casting quality and the operation of sand preparation system. It was soon learned that low moisture contributed to deformed castings. High moisture, on the other hand, caused the sand to aggregate, and produced combustible hydrogen when molten iron entered the sand mold.

Figure 3.4 Moisture Balance for Silica Sand Dry Basis.

CHAPTER FOUR

4.1 Design of Solar Collector

Standard guidelines recommended by the Brace Research Institute for the construction of

Solar cabinet dryers include:

1. An optimal angle of slope for the glazing as a function of the local latitude (applicable to sites both north and south of the equator).

2. The exterior walls should be painted black;

3. The sample trays should be placed reasonably above the cabinet or to ensure a reasonable level of air circulation under and around the product;

4. The top cover glazing should be treated against degradation under UV radiation; and

5. The choice of construction materials should be determined by local availability and the desired level of dryer sophisticate.

4.1.1 Sand Property

The following characteristics of sand were established experimentally and some of their values were taken from the literature.

Table 4.1 Sand Characteristics

Location	Addis Ababa (Akaki)
Product	Moulding silica sand
Sand porosity	40-60%
Bulk density	1500kg/m^3
Initial moisture content(%) wet basis	17.76%
Desired final moisture content(%)wet basis	0.5%
Maximum permissible drying temperature	80 ^{0}c
Ambient relative humidity	60.3%

4.1.2 Design Calculation

The heat gained by the dryer per unit time, Qg is given by [5]

$$Q_d = A_c\left[IN\tau\alpha - U_L\left(T_{ai0} - T_a\right)\right] \tag{4.1}$$

where, A_c= area of transparent cover (m2)

IN= incident insulation (W/m 2)

U_L = overall heat loss for the collector (W /^{0}C)

α = solar absorbance

τ = transmittance

T_{ai0} = temperature of incoming air

Ta = temperature of ambient air

Since the dryer draws the ambient air directly, the last term on the right-hand side vanishes and the rate of energy collection is simply: because temperature of incoming air is equal to temperature of ambient air.

$$Q_d = A_c I\tau\alpha \tag{4.2}$$

If the mass of air leaving the dryer per unit time is m_a, the heat gained by the air Qu is:-

$$Q_u = m_a c_{pa}\left(T_{ao0} - T_{ai0}\right) \tag{4.3}$$

where, C_{pa}= specific heat capacity of air (KJ/kg 0C)

T_{ao0} = temperature of out-going air

A simplified energy equation for the dryer is $Q_d = Q_u$, i.e.

$$Q_d = m_a c_{pa}\left(T_{ao0} - T_{ai0}\right) \tag{4.4}$$

Therefore, the required surface area of the transparent cover, which determines the size and dimensions of the dryer, is obtained from:

$$A_c = \frac{m_a c_{pa}\left(T_{ao0} - T_{ai0}\right)}{I_N\alpha\tau} \tag{4.5}$$

The total energy required for drying a given quantity of sand item can be estimated using the basic energy balance equation for the evaporation of water.

$$M_w h_{fg} = m_a c_{pa} \left(T_{ao0} - T_{ai0}\right) \tag{4.6}$$

where, h_{fg} = specific latent heat of vaporization of water from the silica sand surface (kJ/kg)

Mw = mass of water evaporated from the food item (Kg /s).

The mass of water is estimated from the initial moisture content Mi and the final desired moisture content Mf. The total quantity of moisture to be removed from the silica sand to bring it to the desired moisture from the initial moisture content is used to determine the total mass flow of air required for drying. The quantity of moisture to be removed (Mw) depends on the silica sand and can be found from the following relationship [6].

$$M_w = M_{wc} \frac{\left(M_i - M_f\right)}{100 - M_f} \tag{4.7}$$

where M_{wc}: - is the mass of the wet sand (kg/ s).

During drying, water from the surface of the substance evaporates and water in the inner part migrates to the surface to get evaporated. The ease of this migration depends on the porosity of the substance and the surface area available. Other factors that may enhance quick drying of substances are: high temperature, high wind speed and low relative humidity.

To determine the size of collector and drying bed, it is obvious to know the amount of silica sand that has gone to be dried. Thus the monthly consumption of new silica sand is **$21*10^3$ kg/month** (this figure is taken from ASPSC). So from this value, the annual consumption is:-

$=21*10^3*10$

$21*10^4$ kg/year

In this thesis work 25% of total silica sand is considered for the purpose of evaluation.

Thus $21*10^4*0.25=52.5*10^3$kg/year of silica sand is dried.

Out of these value 15% is clay content which must be removed by water during washing processes. But during this processes mass of silica sand is increased because of mass of

water is added to it when washed by water. Thus mass of new washed silica sand is calculated as:-

If 100 gm washed silica sand goes 82.24 gm dried silica sand (from test conducted on silica sand),the amount of wet sand processes

?x =52.5*10^3kg/year

So x=52.5*10^3*100./82.24

=63837.55kg/year wet sand.

Out of these value 15% is clay content which must be removed by water during washing processes.

X=63837.55kg /year wet sand*0.15 clay content

= 9575.63kg/year of lost due to clay content

Net washed sand = 63837.55-9575.63

=**54262 kg/year**

Daily amount of sand to be dried is 54262/300=**180.9kg/day**

From equation (6.7) the amount of water to be removed is calculated as:-

$$M_w = 180.9\frac{[(17.76-0.5)]}{100-0.5}$$

=31.38kg/day of water to be removed

The total energy required for drying a given quantity of sand items can be estimated using the basic energy balance equation for the evaporation of water is

$$Q_g = M_w h_{fg} \tag{4.8}$$

Where h_{fg} is latent heat of vaporization J/kg which is given by

$$h_{fg} = 4.186 * 10^3 \left(597 - 0.56T_p\right) \tag{4.9}$$

Tp -maximum allowable temperature (80^0c)

h_{fg} =2.43*10^6J/kg

Qg =31.38kg/day* 2.43*10^6J/kg

=76.25MJ/day

Let assume maximum daily sun shine time is 8hr

So energy required per second is

76.25MJ/8*3600s=2647.7J/s

The effective total area surface of the dryer for collecting incident radiation is related to the overall system drying efficiency (η_d), which is given by

$$\eta_d = \frac{M_w h_{fg}}{I_t A_c t} \tag{4.10}$$

Where Ac is the total area of the dryer receiving incident radiation (the total surface area of the primary and secondary collectors), t the total time, h_{fg} the latent heat of vaporization and I_t the intensity of radiation incident on a tilted surface.

The overall drying efficiencies of solar dryers reported in the literature have been shown to vary widely depending on the loading densities and weather conditions .Typical values reported for natural convection solar crop dryer's range from 10% to 15% .To achieve an optimal design, an average overall efficiency value of **12.5%** can be assumed[13].

$$A_c = \frac{M_w h_{fg}}{I_t \eta_d t} \tag{2.11}$$

$$A_c = \frac{76.97MJ/day}{800w/m^2 * 8 * 3600s * 0.125} \quad = \mathbf{26.7m^2}$$

This calculation is done for maximum values of daily solar radiation and sunshine time. This is because, to overcome over size which results in cost reduction.

But as it was stated above the effective area is the total surface area of the primary and secondary collectors. Thus the above result is the sum of primary (collector) and secondary (black wall of chamber) collectors. The dimension of model solar dryer on which experiment was conducted is given as: primary collector is $2m^2$ and secondary collector is $0.5m^2$. Thus the sum is equal to $2.5m^2$. To determine number of such dryer divide the numerical value to the model size of solar dryer. 26.7/2.5=10.68 is number of dryers is required

Therefore the number of such model dryer is approximately eleven (11).

Total size of primary collector =11*2=22m^2

Total size of secondary collector =11*0.5=5.5m^2

4.1.3 Sizing the Solar Dryer (Primary and Secondary Solar Collector)

The solar air heater serves to provide the primary supply of energy to the dryer. Essentially, the absorber within the air heater converts direct and diffuse solar radiation into heat, which is then transferred to the air flowing through it. Taking the ratio of the length of the air-heater (solar collector) to the width as 3:1, which fulfill the length of the cabinet should be at least three times its width to minimize shading effects of the side panels. Thus [5]

$$A_c = L * w$$

But L=3*w

$22 = 3w * w$ Implies that w=2.71m

L= 8.12m

The breadth of the drying chamber, B, is made equal to the width (W) of the air-heater.

Thus, the length of the drying chamber, Ls, is determined from the relation

5.5 = B *Ls, but B=2.71 from above analysis (B=w of collector)

5.5 =2.71*Ls $\Rightarrow$ Ls =2.03m

But the above dimension is reduced by multiplying number of tray in each drying chamber. Thus number of trays were five the size of drying chamber reduced by five times.

The dimension of model solar dryer on which test was conducted given as, length (L=2m) and with (w=1m). For drying chamber dimension is also given as, breadth (B=w=1m) and length (Ls=0.5m).

4.1.4 Area of Drying Bed

The effective drying bed area A_{da} is obtained from first principles by relating the solid density of the wet material to its mass and the corresponding volume as

$$A_{da} = \frac{M_w}{\rho * h_l} \qquad (4.12)$$

Where: - M_w Is the mass of the sand to be dried,

ρ The bulk density of the crop on wet basis,

h_l The layer drying bed thickness,

Determination of h_l The layer drying bed thickness is analyzed as follows

$$volume = \frac{mass}{density} \qquad volume_{total} = \frac{178.4}{1500} = 0.12m^3$$

The above result is total volume of sand be dried. When mass of silica sand for one dryer is 16.22Kg which means the number of model dryer were 11 from above discussion and number of tray is five for each dryer.

Thus the volume of silica sand on each tray is given as [21].

$$volume_{tray} = \frac{16.22}{1500 * 5(numberoftrays)} = 0.0022m^3$$

From model solar dryer A_{da} is $0.4m^2$ (area of tray or drying bed). Thus total bed (tray) area=$11*5*0.4=22m^2$

$$volume_{tray} = A_{tray} * h_l \Rightarrow h_l = \frac{volume}{A_{tray}} = \frac{0.0022}{0.4} = 0.0054m$$

CHAPTER FIVE

5.1 Modeling of Solar Dryer

The transient thermal performance of the solar collector is evaluated by applying energy balance on its components.

The solar radiation energy incident on the collector surface which is inclined at an angle β to the horizontal, defined in terms of the global radiation Gr, the diffuse radiation Dr, the beam radiation factor Rb and the ground reflectivity factor ρ (=0.2), is given by:[1]

$$I_N = R_b\left(G_r - D_r\right) + 0.5(1+\cos\beta)D_r + 0.5\rho(1-\cos\beta)G_r \tag{5.1}$$

Then the flux collected per unit time is calculated as:

$$I_c = I_N\left(\tau_g \alpha_p\right) \tag{5.2}$$

Before calculating all the above formulas let us take some assumption for analysis as follows:

Nearest location= Addis Ababa

Latitude (ϕ) = 9.02^o

Collector facing south (γ) = 0^o

Then starting from equation (5.1) it is clear that the value of I_N is determined after finding each of the necessary components that can be involved inside it as follows.

First calculate the beam radiation factor by using the formula:

$$R_b = \left(\frac{\cos\theta_i}{\cos\theta_z}\right) \tag{5.3}$$

Then find the value of each component to get the whole beam radiation factor as follows.

$$\cos\theta_i = \cos(\phi-\beta)\cos\omega\cos\delta + \sin\delta\sin(\phi-\beta) \tag{5.4}$$

From this the unknowns are the hour angle (ω), declination angle (δ) and the collector slope (β) which is calculated as follows.

$$\omega = (ST - 12) * 15^{o}$$ From equation (2.32)

Where ST=solar time

Then the value of the collector slope is assumed as:

$$\beta = 15^{o}$$

Finally we can find the value of the declination angle for each day of the year starting from day one of the year which is January 1 as n=1.

$$\delta = 23.45 \sin\left(2\pi \frac{284 + n}{365}\right)$$ From equation (2.31)

Then the value of the incidence angle is determined by using the above parameters calculated above.

Then the remaining angle which is going to find is the angle of Zenith by using the following formula, which uses the parameters that was calculated for finding the value of incidence angle.

$$\cos\theta_z = \cos\phi\cos\omega\cos\delta + \sin\delta\sin\phi \quad (5.5)$$

5.1.1 Energy Balance on Each Component of Solar Drier

A solar air heater is a flat plate collector with an absorber plate, a transparent cover at the top and insulation at the bottom and on the sides.

The figure for solar drier looks like this:

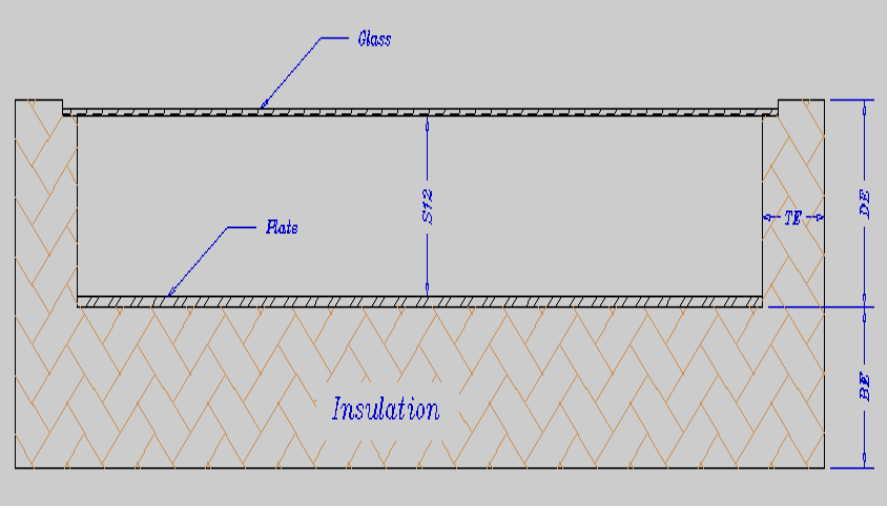

Figure 5.1 Schematic of Diagram Solar Air Heater

Energy balance on the absorber plate, the air stream and the glass cover are performed based on the thermal circuit indicated in section (2.7)

5.1.2 Absorber Plate

Energy balance on the absorber plate is expressed as:

$$\left(mc_p\right)_p \frac{dT_P}{dt} = A_c I_c - A_c U_{pg}\left(T_p - T_g\right) - A_c U_a\left[T_p - \frac{T_{ai} + T_{ao}}{2}\right] - A_c U_{pab}\left(T_P - T_a\right) - A_1 U_{pae}\left(\frac{T_p + T_a}{2} - T_a\right) \quad (5.6)$$

Where $A_1 = p * DE$ -collector perimeter x depth of the edge.

Then the unknown values in the above equation in the following sections can be determined.

U_{pg} = the overall heat transfer coefficients from the plate to the glass by convection and radiation are given by empirical equation as follows:

$$U_{pg} = \left[0.06 - 0.017\frac{\beta}{90}\right]\frac{K_a}{S_{12}} G_{rL}^{1/3} + \varepsilon_{pg}\sigma\left(T_p^{\,2} + T_g^{\,2}\right)\left(T_p + T_g\right) \quad (5.7)$$

Where:- $G_{rL} = \frac{g\beta\left(T_p - T_g\right)}{v^2} L^3$ (5.8)

g=gravitational acceleration

v= kinematic viscosity of the air

The value of β is volume expansion coefficient calculated as

$$\beta = \frac{2}{\left(T_{ai} + T_{ao}\right)} \quad (5.9)$$

A distance between the collector panel and glass cover S_{12} = 0.02 m is the best choice. Then the overall emittance factor ε_{pg} for the absorber plate and the glass cover is obtained from the relation.

$$\varepsilon_{eff} = \frac{1}{\frac{1}{\varepsilon_p} + \frac{1}{\varepsilon_g} - 1}$$ From equation (2.6)

Then the rest are obtained from the standard table by using the equation which is evaluated at the film temperature T_f given by:

$$T_f = \frac{T_{ao} + T_{ai}}{(2)} \tag{5.10}$$

Then the heat transfer coefficient U_a of the air is defined as:

$$U_a = 0.664 \frac{K_a}{L} \left[\frac{P_r G_{rL} \cos\beta}{P_r + 0.9524} \right]^{0.25} \tag{5.11}$$

$$\text{where } P_r = \frac{\nu_a}{\alpha_a} = \frac{c_p \nu}{K_a}$$

Then we have to find the value U_{pab} [heat transfer coefficient from collector plate to air heat transfer coefficient in the bottom side].

$$U_{pab} = \frac{k_{in}}{L_{in}}$$ From equation (2.14)

where:- k_{in} = thermal conductivity insulation.

L_{in} = Thickness of insulation.

Then find the value of U_{pae} [heat transfer coefficient from the plate to the air through the edge].

$$U_{pae} = U_{pab}\left(\frac{A_e}{A_c}\right) \quad \text{, where } A_e = p * t_{BE}$$

Finally if DE=t_{BE} then results in:-

$$A_1 = p * DE = p * t_{BE} \tag{5.12}$$

Due to the transient nature of the radiant and convective heat transfer coefficients, absorber plate energy balance equation is a non-linear equation and its solution requires

an integration scheme that line arises the given differential equation within a given time step.

The plate-temperature at time ($t + \Delta\tau$) is evaluated from available data at time t and incident solar radiation and thermal losses during time interval $\Delta\tau$.

The temperature of the plate at time ($t + \Delta\tau$) in terms of the absorbed useful incident radiation on the surface of the plate, the heat losses through the glass cover and the collector edge, the quantity of heat absorbed by the air stream and temperatures of the collector components at time t is obtained from the absorber plate energy balance equation:

$$T_{p1} = \frac{A_c I_c}{(mc_p)_p}\Delta\tau + \left[1 - \left(\frac{A_c U_{pg}}{(mc_p)_p} + \frac{A_c U_a}{(mc_p)_p} + \frac{A_c U_{pab}}{(mc_p)_p} + \frac{A_c U_{pae}}{2(mc_p)_p}\right)\Delta\tau\right] T_{p0} + \left(\frac{A_c U_{pg}}{(mc_p)_p}\right)\Delta\tau * T_{g0}$$
$$+ \left(\frac{A_c U_a}{2(mc_p)_p}\Delta\tau\right) T_{ao0} + \left(\frac{A_c U_a}{2(mc_p)_p}\Delta\tau\right) T_{ai0} + \left[\left(\frac{A_c U_{pab}}{(mc_p)_p} + \frac{A_1 U_{pae}}{2(mc_p)_p}\right)\Delta\tau\right] T_{a0} \quad (5.13)$$

5.1.3 Air Stream

Considering heat transfer from the collector plate to the air-stream, heat transfer from the air-stream to the glazing and heat transfer to the air entering the collector, energy balance on the stream yields:

$$(mc_p)_a \frac{dT_{a0}}{dt} = A_c U_a \left[T_p - \frac{T_{ai} + T_{ao}}{2}\right] - A_c U_a \left(\frac{T_{ai} + T_{a0}}{2} - T_g\right) - (mfra * c_p)_a (T_{a0} - T_{ai}) \quad (5.14)$$

Where the mass flow rate of air at exit from the collector, $\dot{m}$, is determined from the solar flux collected per unit area, Ic, the temperature difference between the heated air at Tao0 and the ambient (incoming) air temperature at Tai0 as:

$$\dot{m} = \frac{A_C\left(\dot{q}_{ab} - U_L(T_{p0} - T_{a0}0)\right)}{c_{pa}(T_{ao0} - T_{ai0})} \quad (5.15)$$

The temperature of the air stream entering the solar collector at the ambient conditions at time t gains energy from the incident radiant energy on the collector plate. The temperature of the air-stream at outlet from the collector at ($t + \Delta\tau$) is determined from

$$T_{ao1} = \left\{1 - \frac{\Delta\tau}{\left(mc_p\right)_a}\left[A_c U_a + mfra * c_{pa}\right]\right\} T_{a0} + \frac{\Delta\tau}{\left(mc_p\right)_a}\left[mfra * c_{pa} - A_c U_a\right] T_{ai0}$$
$$+ \left[\frac{\Delta\tau}{\left(mc_p\right)_a} A_c U_a\right] T_{p0} + \left[\frac{\Delta\tau}{\left(mc_p\right)_a} A_c U_a\right] T_{g0} \tag{5.16}$$

5.1.4 Glass Cover

Energy balance on the glass cover yields:

$$\left(mc_p\right)_g \frac{dT_g}{dt} = A_c I_N \left[1 - \tau_g\right] + A_c U_{pg}\left(T_p - T_g\right) - A_c U_{ga}\left(T_g - T_a\right) \tag{5.17}$$

The glazing temperature at time t in relation to the absorbed incident radiation on the surface of the glass, the heat losses from the collector plate to the glazing and heat losses from the glazing to the surrounding at time $(t + \Delta\tau)$ is given by:

$$T_{g1} = \frac{A_c I_N \left(1 - \tau_g\right)}{\left(mc_p\right)_g} \Delta\tau + \left\{1 - \frac{\Delta\tau}{\left(mc_p\right)_g}\left[A_c U_{pg} + A_c U_{ga}\right]\right\} T_{g0} + \left[\frac{\Delta\tau}{\left(mc_p\right)_g} A_c U_{pg}\right] T_{p0} +$$
$$\left[\frac{\Delta\tau}{\left(mc_p\right)_g} A_c U_{ga}\right] T_{a0} \tag{5.18}$$

5.2 Energy Balance Equation for the Drying Process

It is needed to find the drop in temperature as the heated air from solar air heater rises through the drying chamber. The vertical blackened sheet absorbs about 20% of solar radiation [2].

5.2.1 Heat and Mass Balance on the First Tray of Drying Chamber

$$(m_a c_p)_a (Tao1 - Td) + 0.2 A_d I_N = M_{w1} h_{fg} \tag{5.19}$$

The temperature of the air stream out going from first tray of the drying chamber at the ambient conditions at time $(t + \Delta\tau)$ gains energy from the incident radiant energy on the collector plate and black wall of drying chamber in the first tray is determined from:

$$Td = Tao1 - \frac{M_{w1} h_{fg}}{(m_a c_p)a} * \Delta\tau + \frac{0.2\alpha A_d I_N}{(m_a c_p)a} * \Delta\tau \tag{5.20}$$

5.2.2 Heat and Mass Balance on the Second Tray of Drying Chamber

$$(m_a c_p)_a (Td - Tr) + 0.2 A_d I_N = M_{w2} h_{fg} \tag{5.21}$$

The temperature of the air stream out going from second tray of the drying chamber at the ambient conditions at time ($t + \Delta\tau$) gains energy from the incident radiant energy on the collector plate and black wall of drying chamber in the second tray is determined from:

$$Tr = Td - \frac{M_{w2} h_{fg}}{(m_a c_p)a} * \Delta\tau + \frac{0.2\alpha A_d I_N}{(m_a c_p)a} * \Delta\tau \tag{5.22}$$

5.3 Equilibrium Moisture Content

The equilibrium moisture content (EMC) is the moisture content at which the silica sand is neither gaining nor losing moisture; this, however, is a dynamic equilibrium and changes with relative humidity and temperature.

The rates of moisture desorption from the product to the environment and absorption from the environment is in equilibrium, and the silica sand moisture content at this condition is known as the equilibrium moisture content. The equilibrium moisture content (*M*e) is the Chung-Pfost equation taken from the ASAE Standards and is given by [12]:

$$M_e = 0.33872 - 0.05897 \ln((\theta + 30.205) \ln(RH)) \tag{5.23}$$

Where; - θ is silica sand (grain) temperature

RH Is relative humidity

Figure.5.2 determination of moisture content of silica sand experimentally

During drying, water at the surface of the silica sand evaporates and water in the inner part migrates to the surface to get evaporated. The ease of this migration depends on the porosity of the silica sand and the surface area available. Other factors that may enhance quick drying of sand are: high temperature, high wind speed and low relative humidity.

CHAPTER SIX

6.1 Simulation of Solar Dryer Using Matlab

Simulation of plate temperature, glass temperature, air temperature and mass follow rate of solar dryer for selected (representative days of) months was simulated by mat lab software as shown in the following figures.

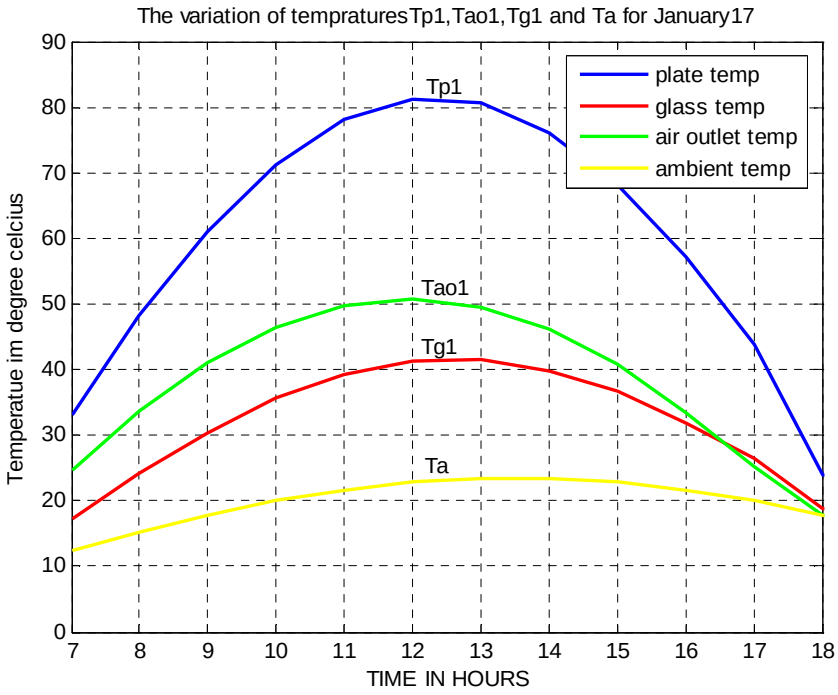

Figure 6.1 Variation of Temperature of Plate, Glass and Air of Model Solar Dryer for January 17

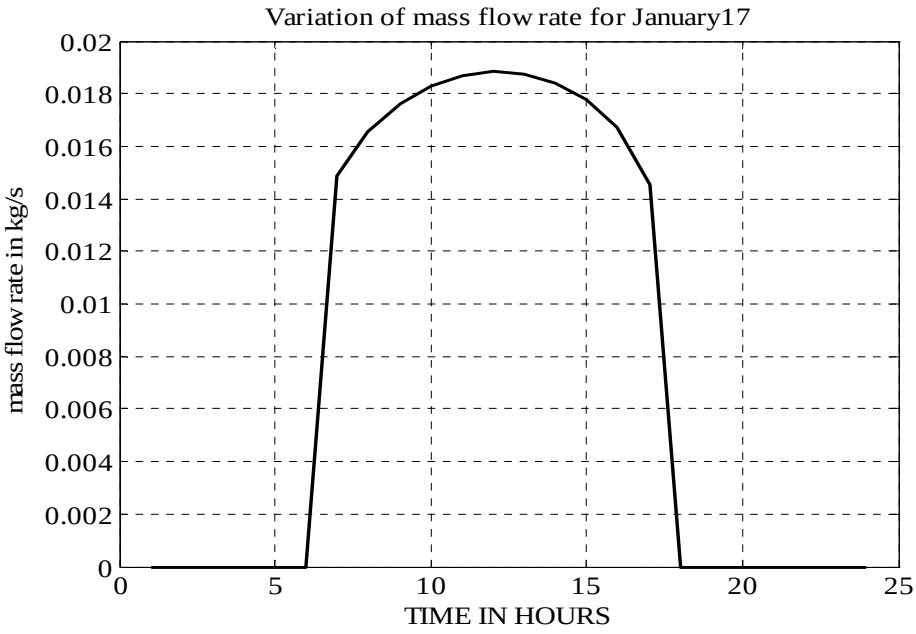

Figure 6. 2 Variation of Mass Flow Rate of Model Solar Dryer for January 17

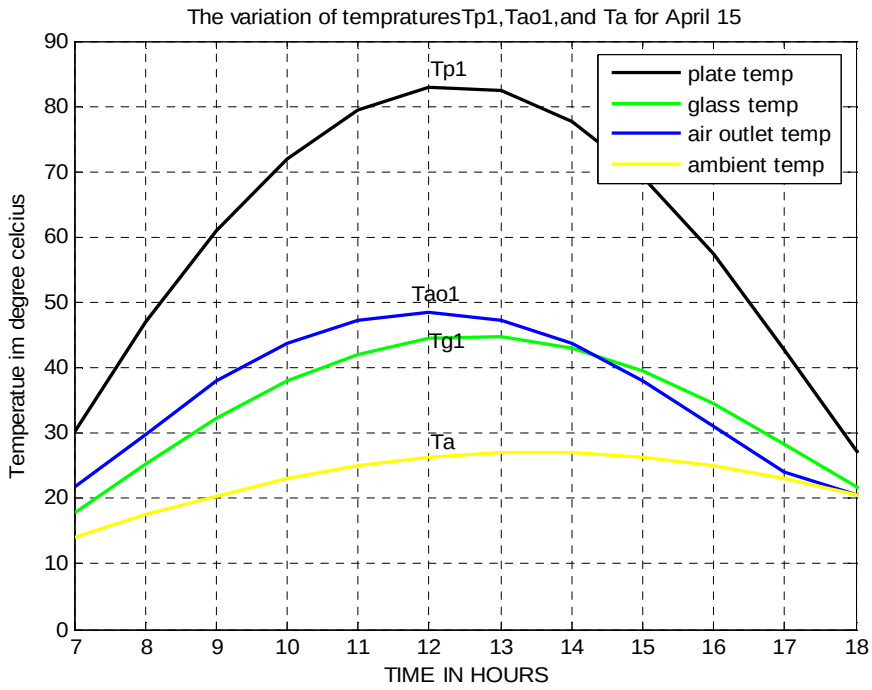

Figure 6.3 Variation of Temperature of Plate, Glass and Air of Model Solar Dryer for April 15.

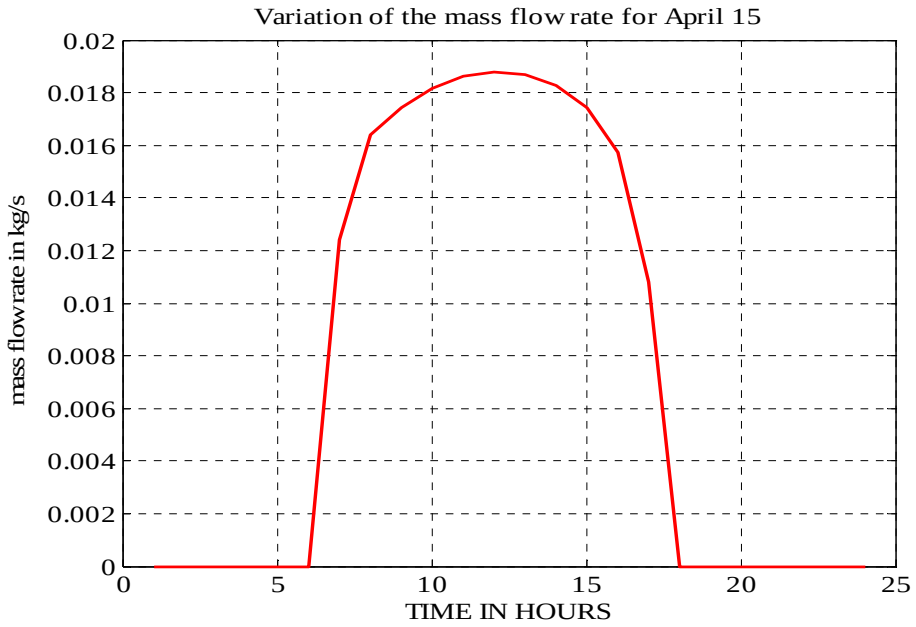

Figure 6.4 Variation of Mass Flow Rate of Model Solar Dryer for April 15

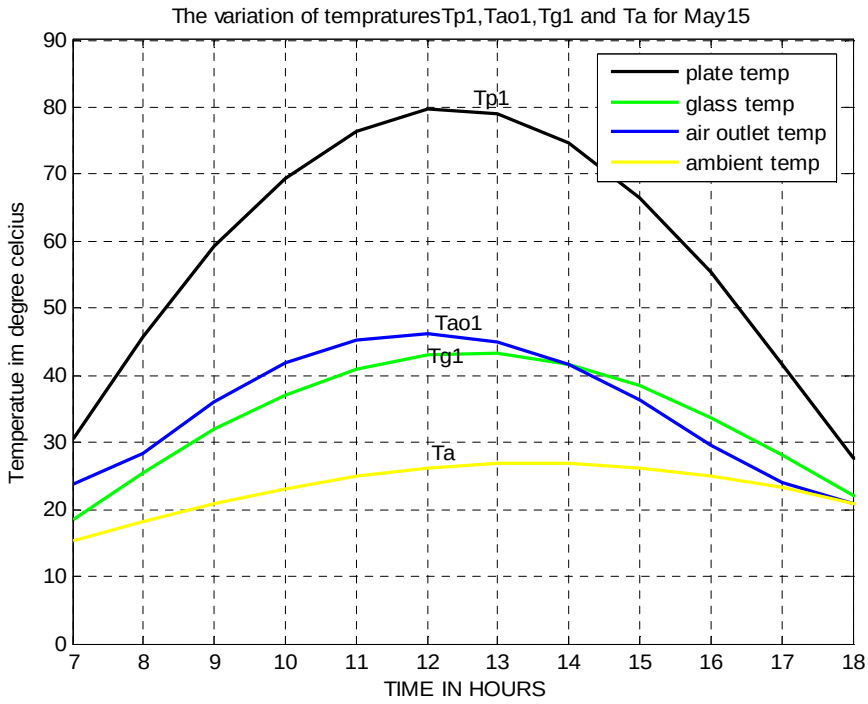

Figure 6.5 Variation of Temperature of Plate, Glass and Air of Model Solar Dryer for May 15

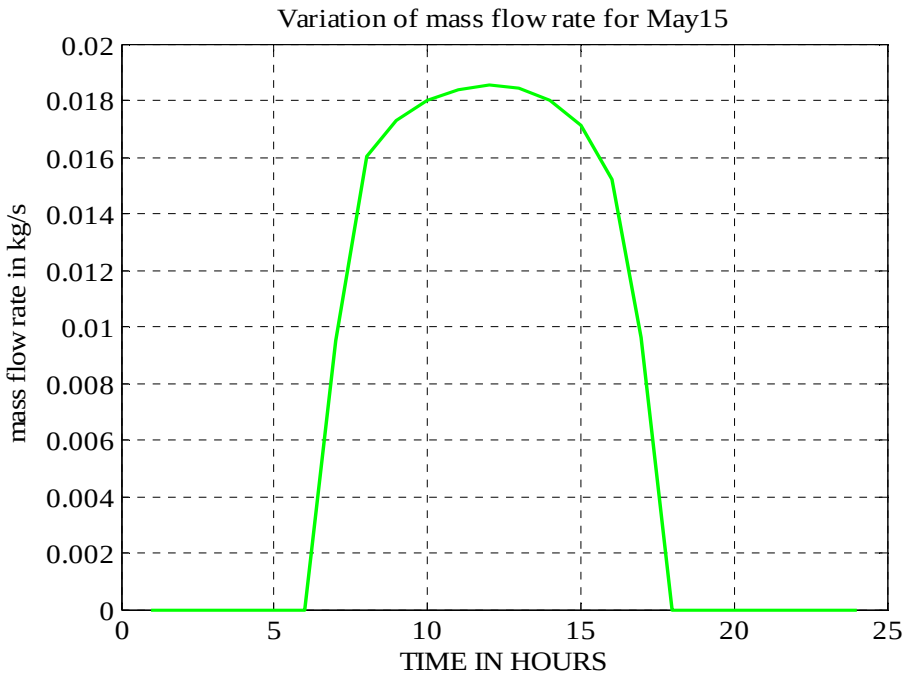

Figure 6.6 Variation of Mass Flow Rate of Model Solar Dryer for May 15

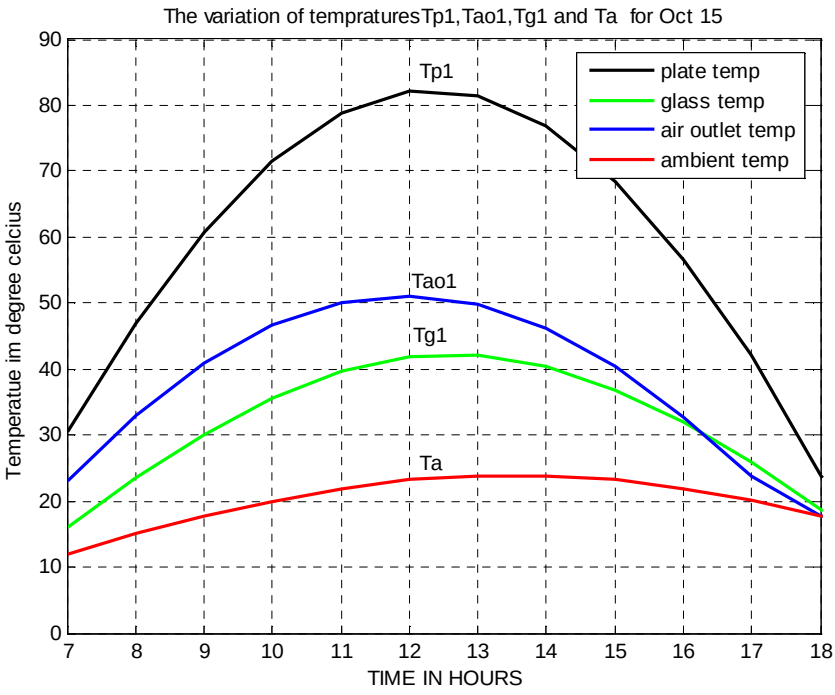

Figure 6.7 Variation of Temperature of Plate, Glass and Air of Model Solar Dryer for Oct 15

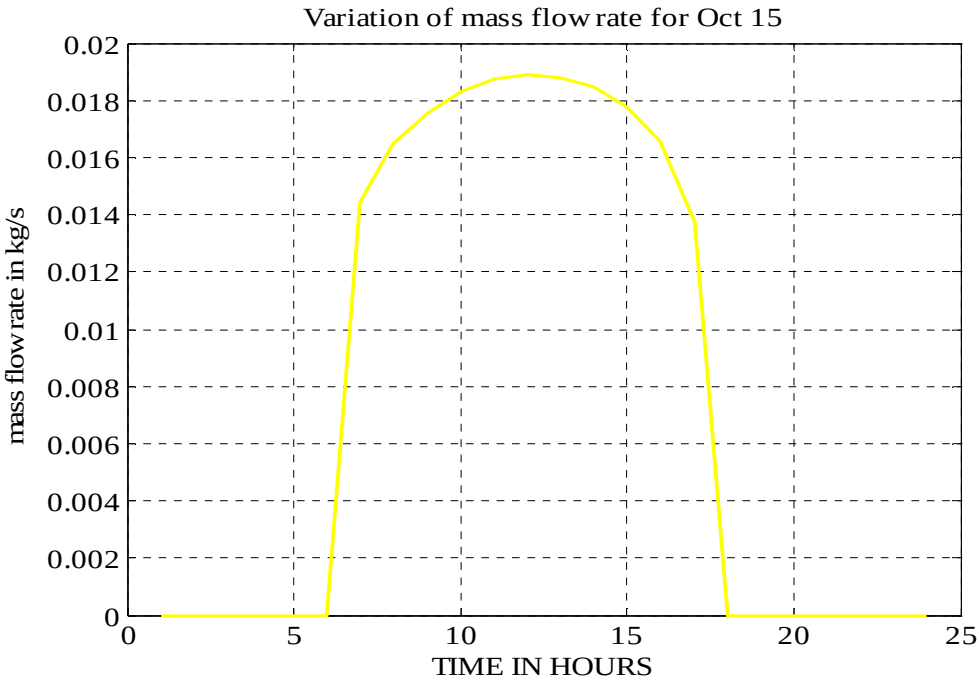

Figure 6.8 Variation of Mass Flow Rate of Model Solar Dryer for Oct 15

CHAPTER SEVEN

Experimental Setup and Instrumentation

7.1 Instruments

To investigate effects of environmental and operating parameters on the performance of the dryer, various measuring devices were used [2].

1. **Pyranometers** were placed on the solar collectors to measure solar radiation on the south-facing side of the collector.

2. **Thermocouples** of type K were used to measure air temperatures in the inlet air to the dryer, out let air ducts and drying chambers.

3. **Hot wire anemometers** were employed to monitor the air speed in the collector and in the air ducts. This anemometer was also used to monitor the ambient wind speed.

4. **Hygrometer** – were used to measure relative humidity of ambient air and drying air periodically.

But in this test only thermocouple were used for measuring temperature and the rest measurement was taken from metrology nearest location for the site (Addis Ababa).

7.2 LabVIEW

LabVIEW is a graphical programming language that uses icons instead of lines of text to create applications. In contrast to text-based programming languages, where instructions determine program execution, Lab VIEW uses dataflow programming, where the flow of data determines its execution [24].

1 How Does LabVIEW Work?

Every Lab VIEW program (VI) uses functions that manipulate input from the user interface or other sources and display that information or move it to other files or other computers.

2 Data Flow

Lab VIEW follows a dataflow model for running VIs. A block diagram node executes when all its inputs are available. When a node completes execution, it

supplies data to its output terminals and passes the output data to the next node in the dataflow path as shown in block diagram.

supplies data to its output terminals and passes the output data to the next node in the dataflow path as shown in block diagram.

7.2.1 A VI Contains the Following Three Components

1. **Front Panel**:-Interactive user interface of a VI. Front panel appearance imitates physical instruments, such as oscilloscopes and multimeters. The following figure shows the font panel of Lab VIEW which helps the user to check or to see how reading is going on.

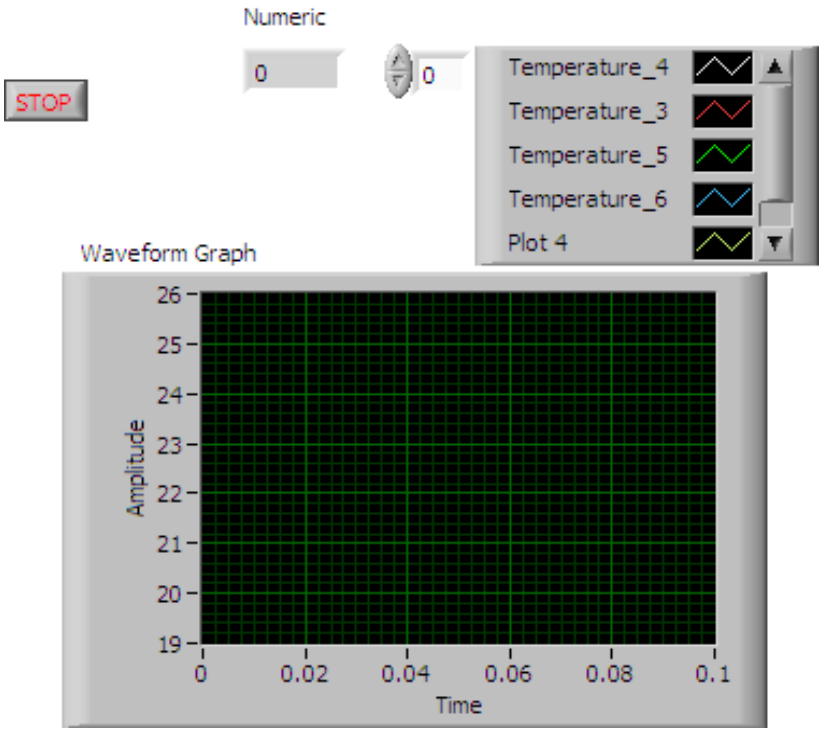

Figure 7.1 The Front Panel of Lab VIEW

2 **Block Diagram**:-Pictorial description or representation of a program or algorithm. The block diagram consists of executable icons called nodes and wires that carry data between the nodes. The block diagram is the source code for the VI.

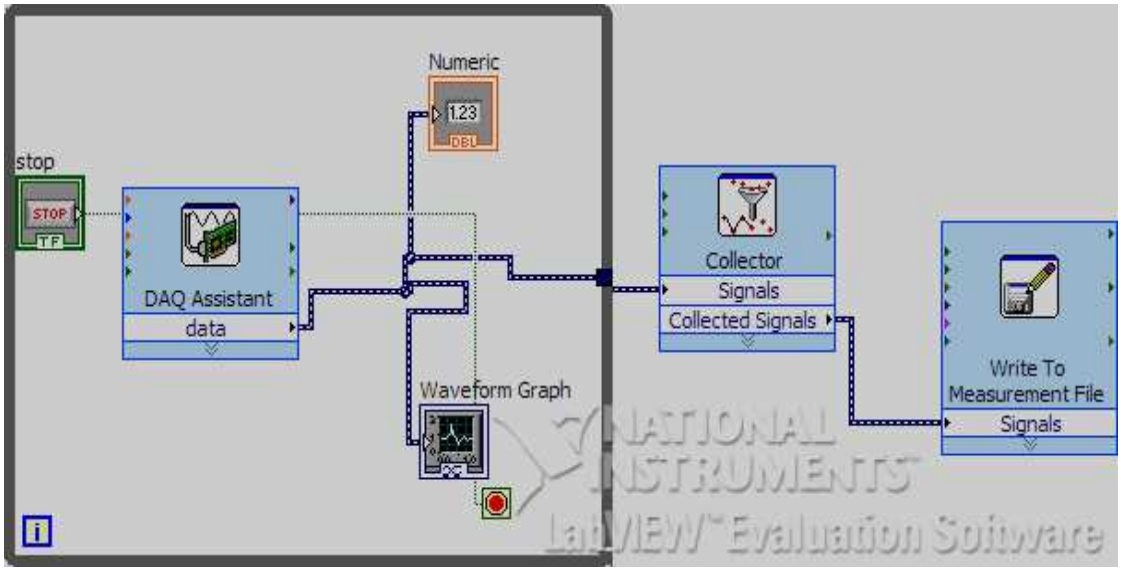

Figure 7.2 The Block Diagram of Lab VIEW

3 **Icon and connector pane**

Connector Pane:-Region in the upper right corner of a front panel or block diagram window that displays the VI terminal pattern. It defines the inputs and outputs you can wire to a VI.

Icon: - Graphical representation of a node on a block diagram.

7.3 Experimental Set Up of Solar Dryer

Outer side black painted steel sheet of 0.8 mm thick and 4 mm thick glass were used for the construction of the chamber body. The solar collector is parallel piped shape with dimension of L=2 m x W =1 m x 0.14 m having 80 mm channel depth, 20 mm gap between the absorber plate and glass, and on the bottom 20 mm thick fiber glass insulation. The collector is inclined at an angle of 15^0 with the horizontal. The absorber plate consists of 1 mm thick steel flat sheet blackened on the sun facing side. The cover material of the collector is 4 mm thick commercial glass [22].

Drying chamber: - in side drying chamber five numbers of trays were prepared. The trays were manufactured from aluminum sheet metal. The size the trays were length (L=0.96m) and width (w=0.4m) which is less than the inside dimension of drying chamber. Since the trays were not in wire mesh form (it is flat aluminum sheet metal) the air is forced by natural convection to flow through the trays in zigzag fashion. The following figure shows how trays were placed in drying chamber.

Figure 7.3 Picture Which Shows How Trays Were Placed in Drying Chamber

7.4 Sensors Positioning

To conduct an experiment the sensors are positioned at right place in right time for right purpose. Thus the following figure shows how sensor is located on the dryer to collect the information that was needed.

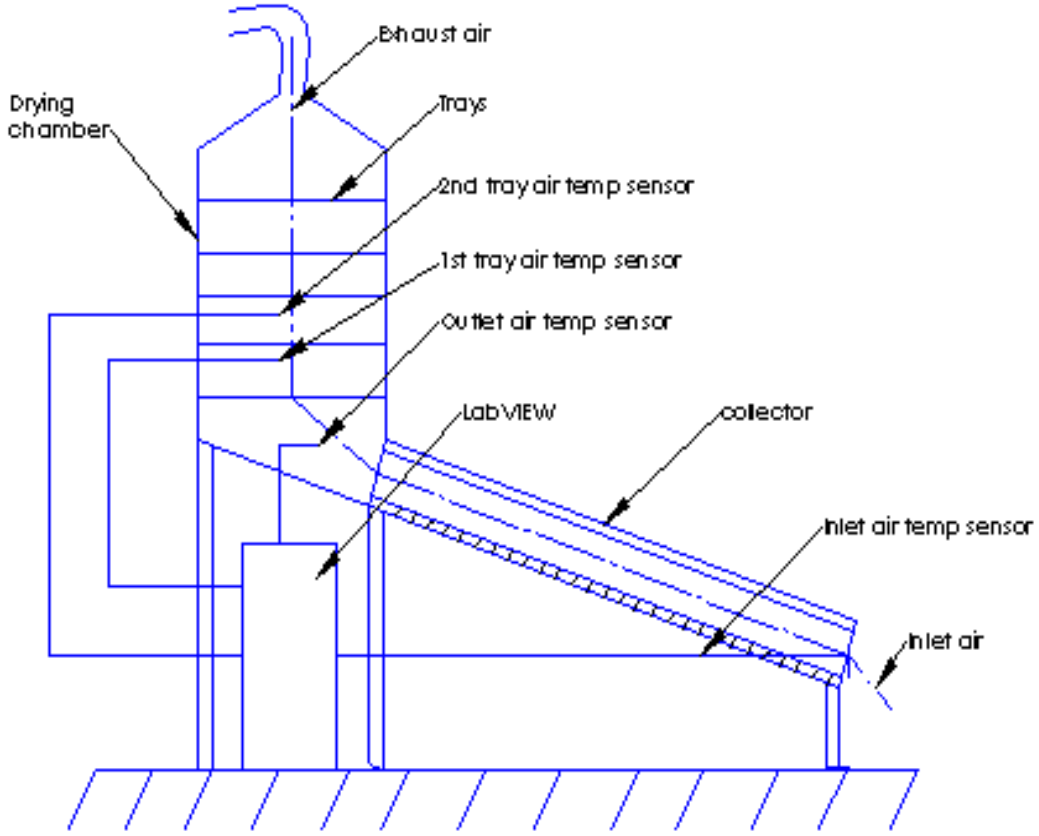

Figure 7.4 Schematic Diagram of Sensor Positioning for Experimental Set Up.

7.5 Experimental Procedure

The daily drying rate was estimated by measuring the weight loss of the product after each day of drying. The relative humidity and solar radiation data was obtained from Addis Ababa metrology. The working procedure adopted for taking the observations is as follows.

1. Solar dryer orientation was set with its solar air heater facing south.
2. The product was loaded in three trays in the drying chamber at 10.00AM hours. The doors of the drying chamber were closed.
3. Readings were taken at intervals of 1 min (from 10 AM to 5 PM) in the following sequence:
   - Inlet air temperature of solar dryer Outlet temperature of solar dryer and
   - Variation of temperature in drying chamber
4. The above readings were noted in a specially prepared datasheet (excel).
5. The final readings were taken at 5 PM. The product was then removed from the drying chamber, taken in plastic bags and their weight was noted.

6. The experiments were performed with new silica molding sand until they were reduced to safe moisture level, which is favorable for molding application.

7.6 Experimental Result and Discussion

7.6.1 Air Temperature Variation in Drying Chambers.

The test was conducted on three trays. The first tray (lower tray) was positioned at 0.01m from insulation and the rest tray positioned at the same distance (0.01m) above each other. The percentage weight reduction in mass of silica sand was greatest when spacing between trays was minimum as much as possible.

The following figures shows varaition output temperature of drying chamber and inlet (ambient temperature to dryer) and outlet (inlet air temperature to drying chamber) air temperature of solar dryer.

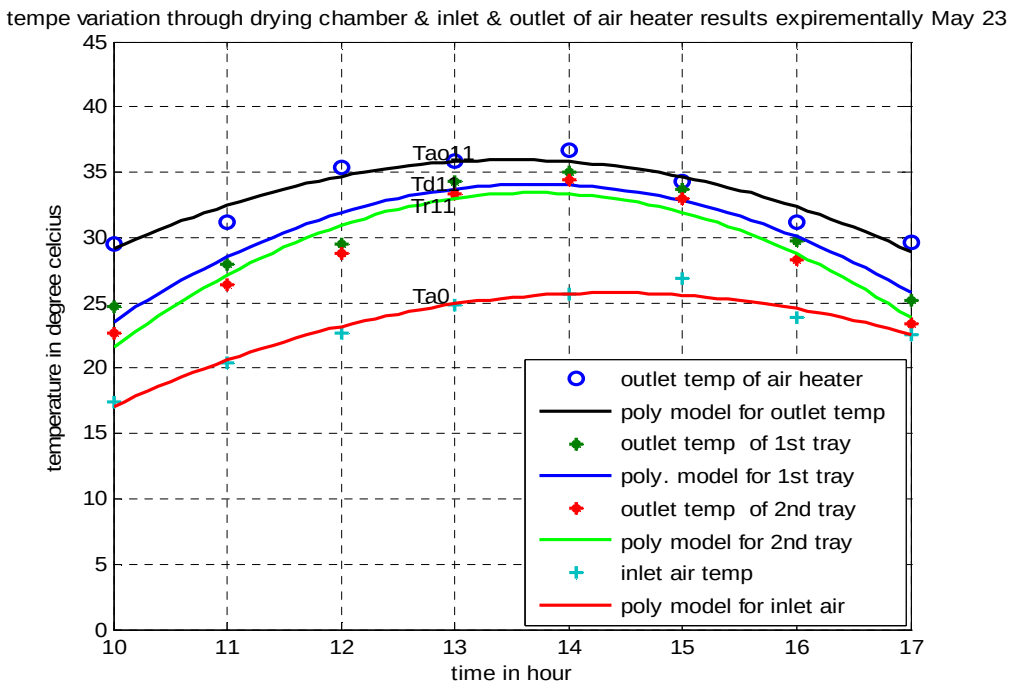

Figure 7.5 Temperature Variation through Drying Chamber and Inlet and Outlet of Air Heater Results Experimentally on May 23.

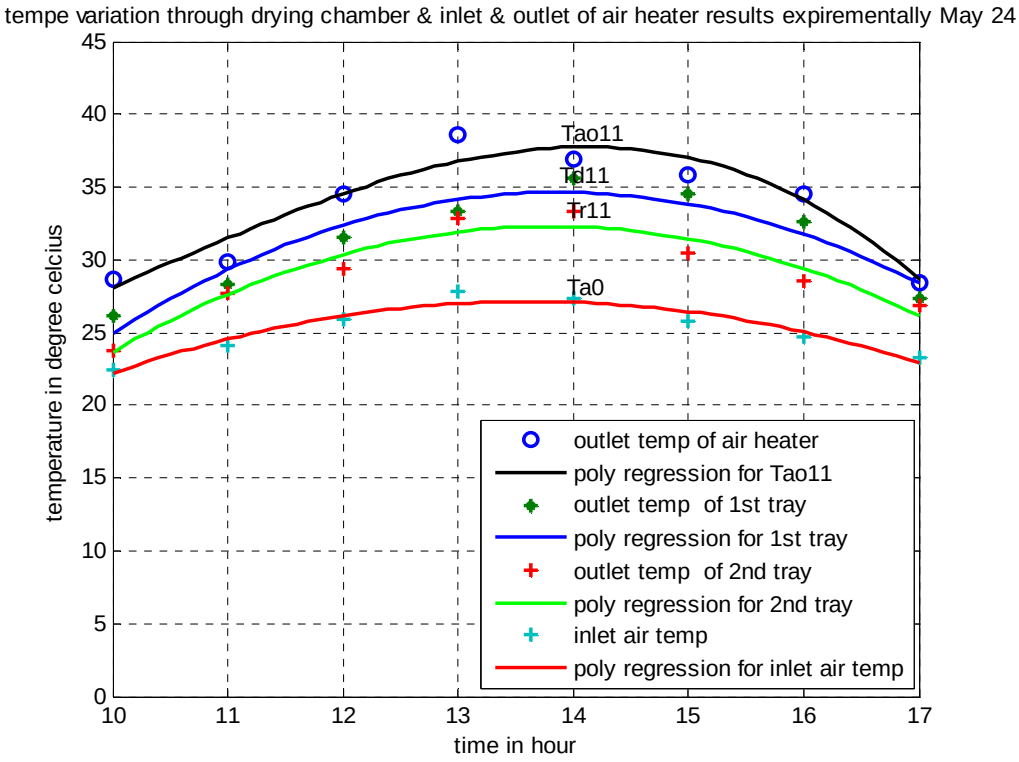

Figure 7.6 Temperature Variation through Drying Chamber and Inlet and out let Air Heater Results Experimentally on May 24.

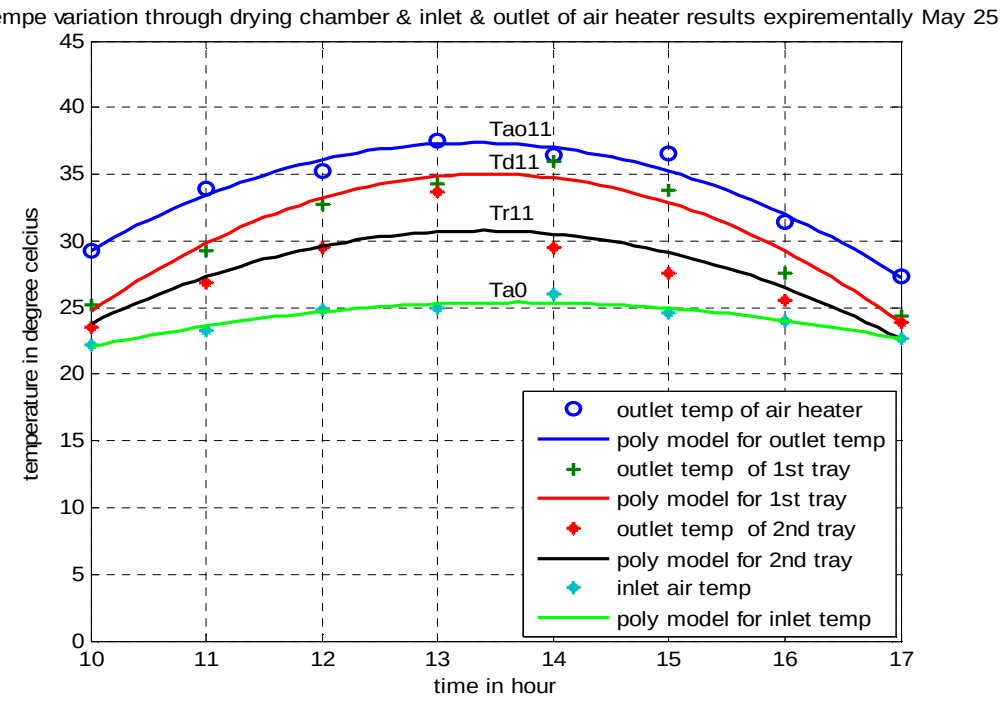

Figure 7.7 Temperature Variation through Drying Chamber and Inlet and Outlet of Air Heater Results Experimentally on May 25.

Discussion

As observed from the above figures it was clearly indicated that the temperature variation through drying chambers and inlet (ambient temperature to dryer) and outlet (inlet air temperature to drying chamber) air temperature of solar dryer. This means

1. Outlet temperature (inlet air temperature to drying chamber) is higher because of incoming air temperature to the drying chamber is heated by solar radiation in the air heater and additionally heated by the vertical blackened wall of the drying chamber, which is exposed to solar radiation.

2. Outlet temperature of first tray is lower than outlet temperature (inlet air temperature to drying chamber) because it absorbs moisture from silica sand loaded on first tray.

3. The outlet temperature of second tray is lower than the first tray temperature because since it absorbs moisture of silica sand which is loaded on the second tray.

4. Finally it was concluded from the above result that the temperature is lowers upraise through drying chamber and also drying rate (decrease) and drying period (increase). This is due to temperature variation through drying chambers.

1. Comparison Between Experimental and Theoretical Result

The following figures indicate the comparison between experimental and theoretical results for the selected days. These figures shows that test was conducted on inlet and out let temperature of solar air heater and variation of temperature of drying chamber in each trays.

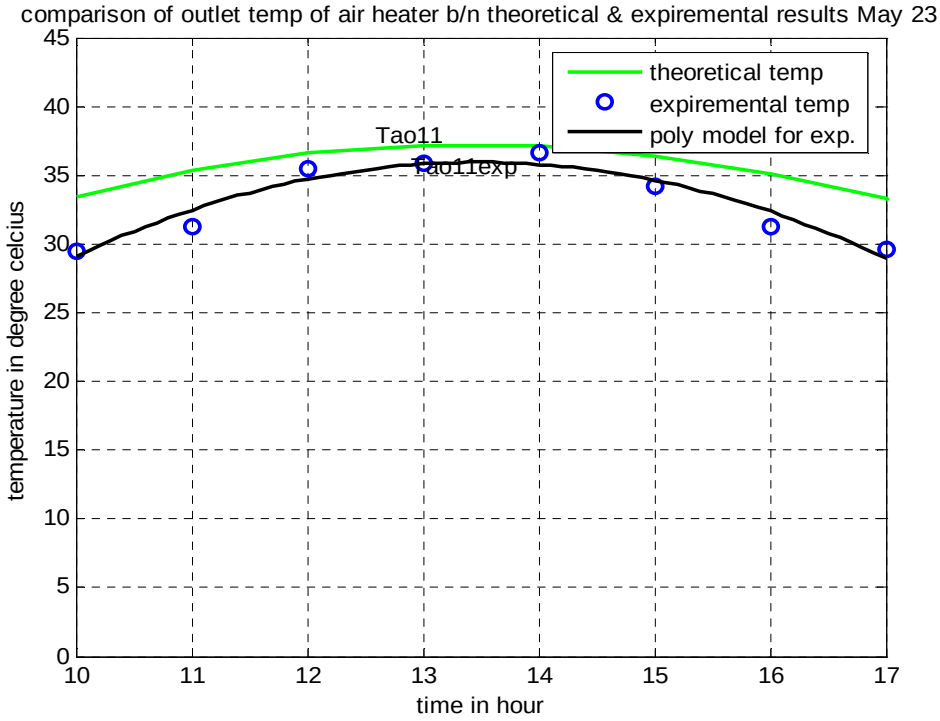

Figure 7.8 Comparisons between Experimental and Theoretical Result of Outlet Temp of Solar Air Heater May 23**.**

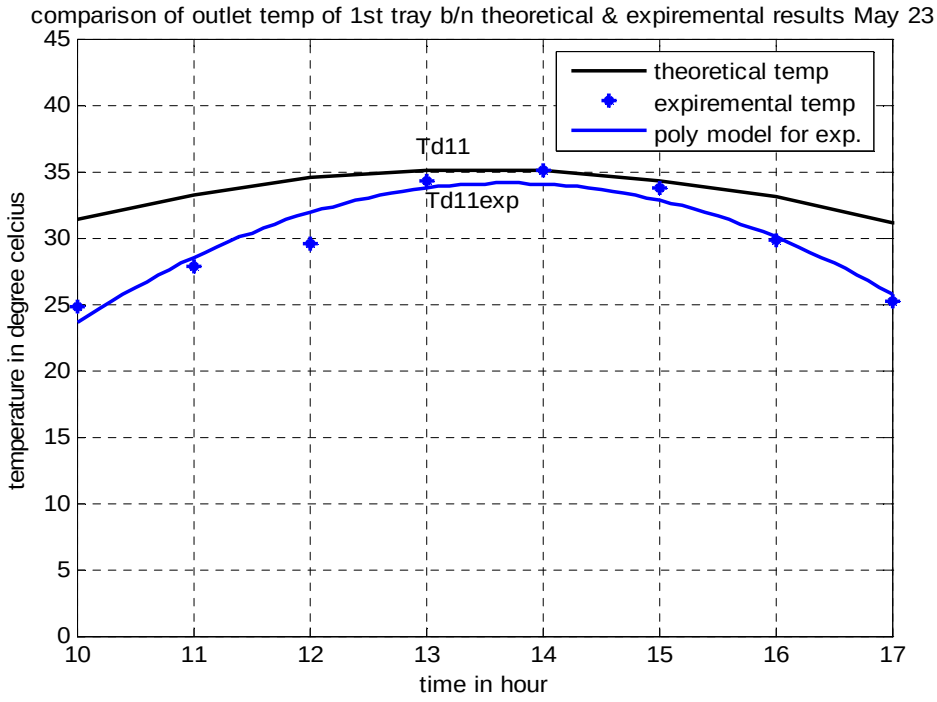

Figure 7.9 Comparisons between Experimental and Theoretical Result of Outlet Temp of First Tray May 23.

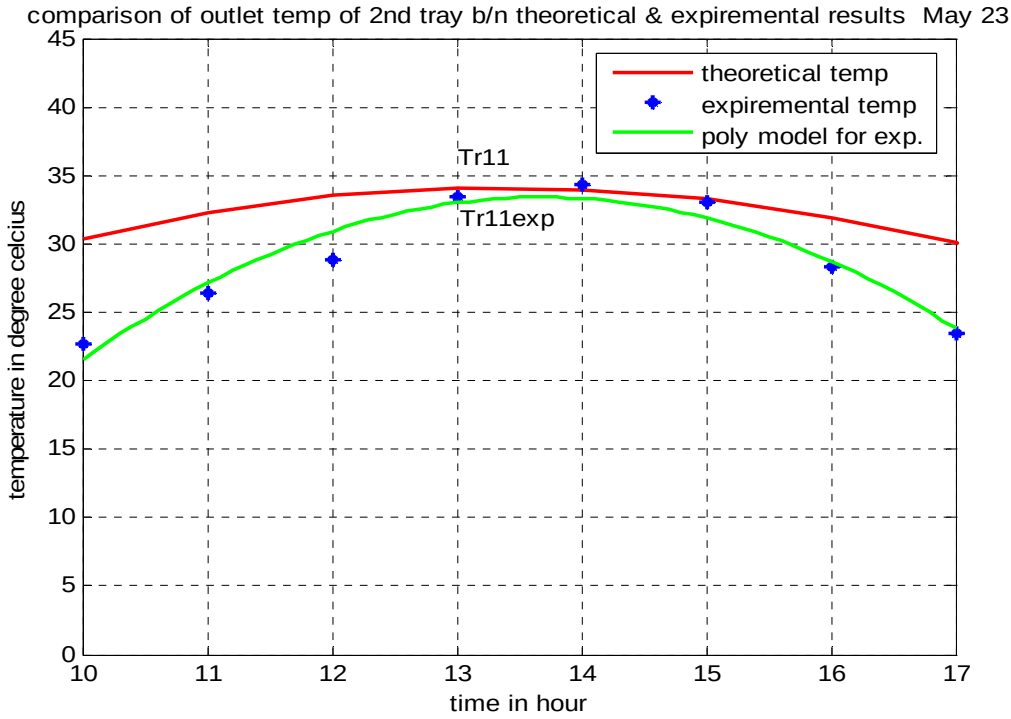

Figure 7.10 Comparison between Experimental and Theoretical Result of Outlet Temp of Second Tray May 23.

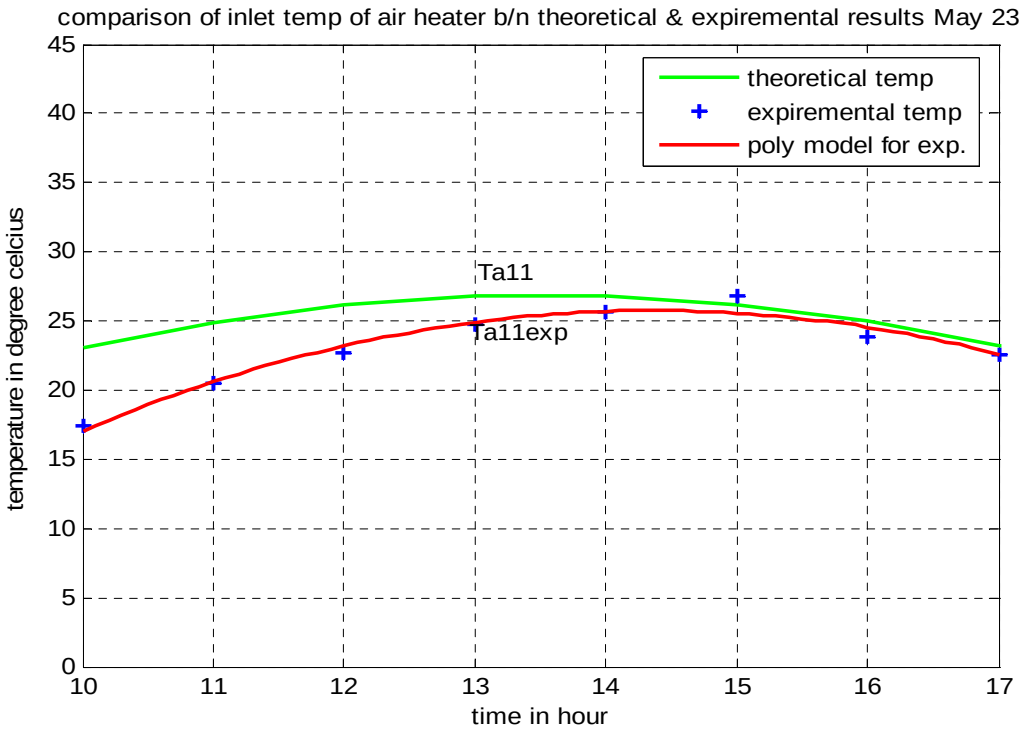

Figure 7.11 Comparisons between Experimental and Theoretical Result of Inlet Temp of Solar Air Heater May 23.

Discussion

1. From the result it is also observed that the theoretical temperature is higher than experimental temperature, this is because of the losses that were considered in the theoretical part is less, because it is difficult to apply these losses as it is in the practical case (losses occur during manufacturing).

2. In actual case once the drying chamber attain high temperature, it maintain its temperature even when outside temperature drops, for some time period. Because the heat is absorbed by chamber and even by the sample that was placed in the chamber to dry. But in theoretical case this situation can't be attained.

3. The variation of temperature between experimental and theoretical is not much significant as shown in the figure above.

7.6.2 Mass of Moisture Removed

The dryer was loaded with silica sand (0.54 mm drying bed thickness) and its weight was measured at the start when it was loaded at 10.00AM and final weight was measured at 5.00PM. The weight loss was used to calculate the moisture removed in Kg water/Kg dry matter at intervals as the silica sand dried. It was observed (from figure below) that the moisture removal decrease due to decrease in temperature in drying chamber from bottom to top of trays.

This is because of air evaporates moisture from the product. This lowers the temperature of the air and finally results in low moisture removal of upraise of drying chamber [2, 3].

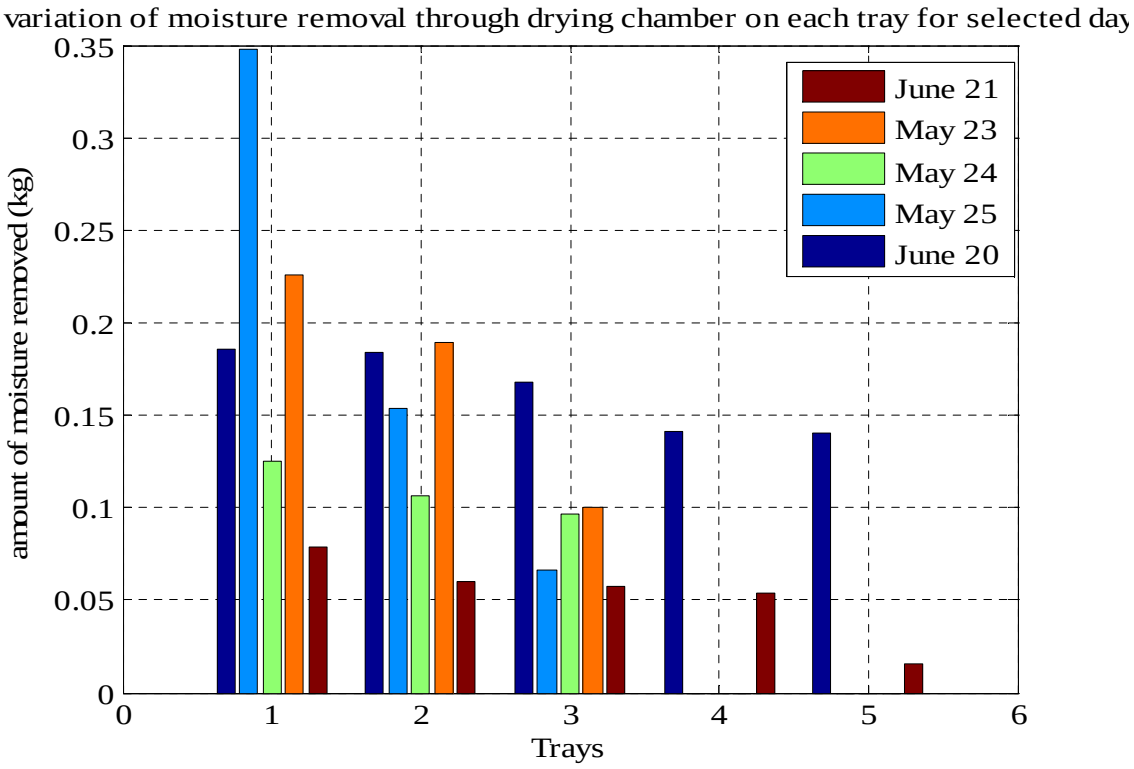

Figure 7.12 Mass of Moisture Removed Experimentally (Kg/day) of Drying Chamber for the Selected Days on May 23, 24 and 25, June 20 and 21.

7.6.3 Moisture Content

Moisture content (Mc) is the quantity of water contained in silica sand (called sand moisture). Water content is used in a wide range of scientific and technical areas, and is expressed as a ratio, which can range from 0 (completely dry) to the value of the materials' porosity at saturation. And it is also a measure of wetness or dryness of silica sand. It can be calculated on either a wet or dry basis. The wet basis moisture is the ratio of mass of water in silica sand to wet mass of the sample that is [17].

$$M_{cw} = \frac{M_w - M_d}{M_w} \tag{7.1}$$

The dry basis moisture is the ratio of the mass of water in silica sand to the mass of the dry matter, that is:

$$M_{cd} = \frac{M_w - M_d}{M_d} \tag{7.2}$$

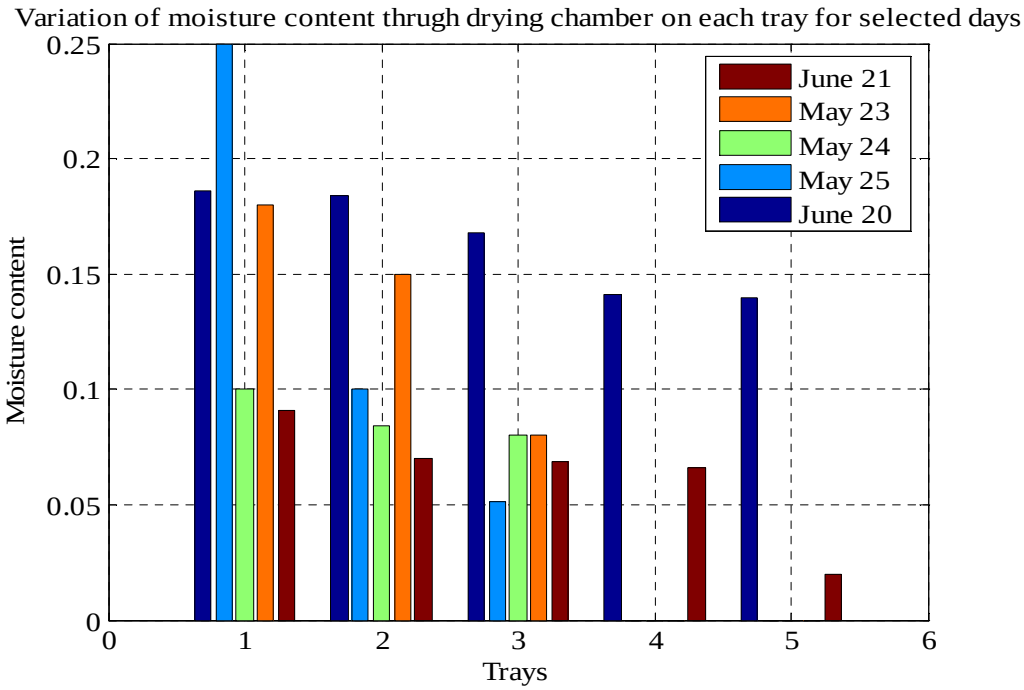

Figure 7.13 Variation of Moisture Content through Drying Chamber on each Tray for Selected Days (May 23, 24 and 25 and June 20 and 21).

7.6.4 Drying Rate

Drying rate is a rate of mass transfer process consisting of the removal of water moisture or moisture from another solvent, by evaporation from solid, silica sand. To be considered "dried", the final product must be solid as powder form in silica sand.

Drying rate, which is the quantity of moisture removed from the product in a given time, was computed numerically as:

$$\frac{dM}{dt} = \left(\frac{M_i - M_f}{t} \right) * 100 \tag{7.3}$$

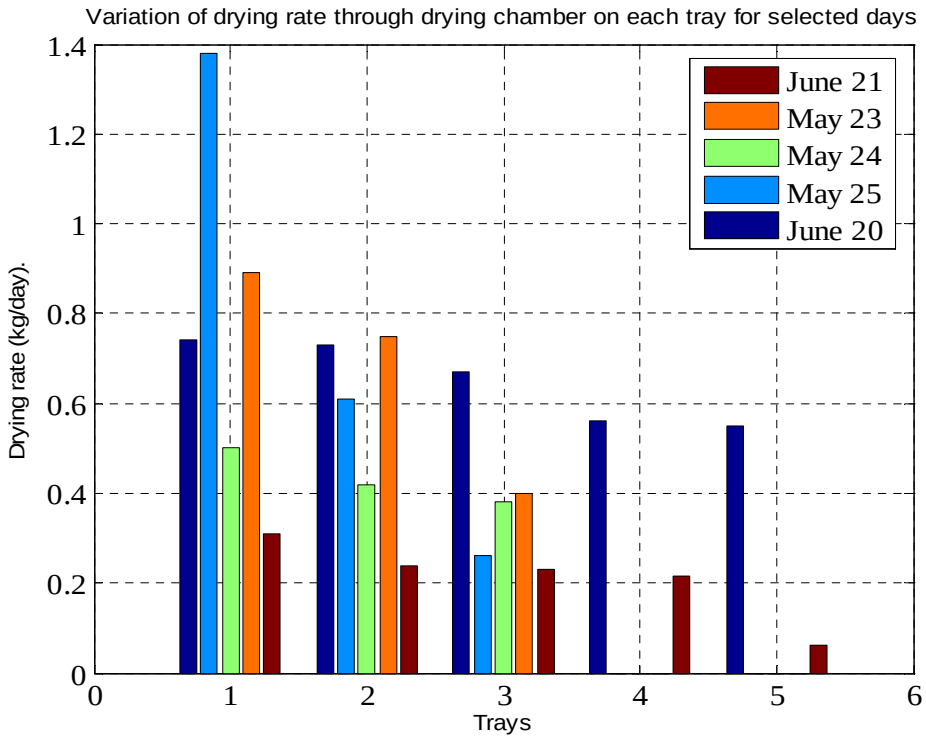

Figure 7.14 Variation of Drying Rate through Drying Chamber on each Tray for Selected Days.

7.6.5 Drying Efficiency

The drying efficiency was defined as the ratio of amount of heat needed to evaporate the moisture content in the silica sand in one day to the solar radiation falling on the solar dryer. The efficiency was calculated for all the tests conducted.

Which is given by (from eqeution 6.10)

$$\eta_d = \frac{M_w h_{fg}}{A_c I_t t} * 100 \qquad (7.4)$$

Where: - M_w is mass of moisture removed

h_{fg} is latent heat of vaporization of water

A_c area of solar collector

I_t total solar radiation incident on absorber and

t is time.

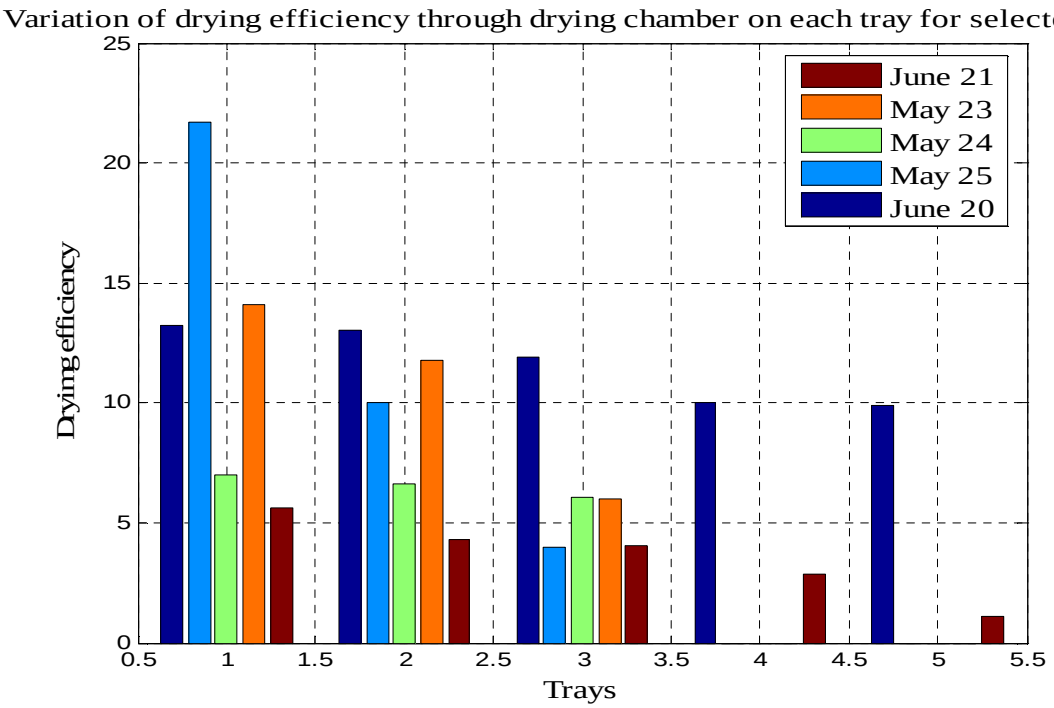

Figure 7.15 Variation of Efficiency through Drying Chamber on each Tray for Selected Days (May 23,24and25, June 20 and 21)

Discussion

1 The mass of moisture removed were varies from one tray to another tray. This variation is due to temperature variation through drying chamber. As discussed previously, temperature is decrease through upraise of drying chamber, which affect moisture removal. Therefore moisture removal is directly depends on the temperature of the air.

2 The sun dried control samples were weighed for comparison (Initial mass= 1.402Kg, Final mass =1.248Kg.Then amount of moisture removed per day on open sun were 0.154Kg). When compared from this result with dryer it is less efficient. .

3 But in the rest of the days it was observed that drying rate, moisture content, moisture removed and drying efficiency decrease from bottom trays to the top as result of temperature variation through drying in upraise motion.

4 Finally it was concluded from the above result that the temperature is lowers upraise through drying chamber and also drying rate (decrease) and drying period (increase). This is due to temperature variation through drying chambers.

CHAPTER EIGHT
Feasibility Analysis

8.1 Introduction

Although the resource of a solar energy system, that is, the solar irradiation, is free, the equipment required to collect it and convert it to useful form (heat or electricity) has a cost. Therefore, solar energy systems are generally characterized by high initial cost and low operating costs. Thus, the economic problem is to compare an initial known investment with estimated future operating costs, including both the cost to run and maintain the solar energy system and auxiliary energy used as backup. A cost analysis based on the local market conditions was made to estimate the value addition to the product, by the solar dryer (Schirmer et al., 1995) [8].

Since the availability of solar energy is intermittent and unpredictable, it is generally not cost effective to provide 100% of the energy requirements of a thermal system with solar energy year round. This is because, when the system satisfies fully the requirements under the worst operating conditions, it will be greatly oversized during the rest of the year, requiring the dumping of thermal energy, which is not cost effective.

8.2 Life Cycle Costing

In life cycle analysis, both the initial cost and the annual operating costs are considered for the entire life of the solar energy system. In this thesis primarily initial cost and operating were considered.

8.2.1 Initial Cost

Initial Costs are necessary to prepare the project for service. These costs include the purchase price, installation costs and charges for engineering work that must be done

Table 8.1 Equipment Cost for Model Solar Dryer

No		Part list	Dimension (unit)	Thickness(mm)	Quantity	Total cost(birr)
1	Purchase cost or material cost	Glass cover	1*2(m2)	5.0	1	260
		steel sheet plate	1*2(m2)	0.8	3	960
		Silicon rubber	bottle spray		2	140
		Black paint	kg		1	70
		Bolton and nut	M6		26	50
		Legs (RHS)	Dia=30*30[mm2]	2.0	1	245
		Skeleton (RHS)	Dia=20*20[mm2]	1.5	1	140
		Aluminum sheet	1*2(m2)	0.8	1	300
		Insulation cost (fibber glass)	1*1.2(m2)	25	2	640
2	Installation costs					-
3	Engineering Cost					-
						2805

In order to obtain 178.4Kg/day dried silica sand, the total cost required was estimated as follow. Initial cost for model drier was 2805ETB and eleven (11) such drier were required to dry the required amount of silica sand therefore cost of drier will be (11*2805=30855ETB). Installation cost and Engineering cost are neglected because of it doesn't require any additional cost since it was done by their employers that have their own salary.

8.2.2 Operating Cost

Utilization (operating) costs are those required on a routine basis for operating and maintaining the project. These include maintenance (replacement of broken glass). Operating costs can be direct or indirect. Direct costs include labor and materials for routine maintenance. Indirect costs are the costs not directly attributable to the project, but in this work indirect cost was ignored because this work doesn't require any supervisor, and cleaning supplies.

Table 8.2 Operating Cost for Model Solar Dryer

Operating cost	Direct cost	Labour	200birr
		Material	500birr
	Indirect cost	Salaries for supervisor	-
		Cleaning cost	-
Total			700birr

8.2.3 Cost Saving

As calculated in design part of this work the total energy required to dry the given amount of silica sand per day is 76.25MJ/day. In a day dryer works for eight (8hr) hours thus the amount of power in kilowatt hour is given as:-

Power=energy/time (8hr)=$76.25*10^6$MJ/8*3600=26.48KWhr

If this energy is supplied from EPCO, it charges cost per day according to the KWhrs ranges.

Data collected from EPCO for self contained systems- industrial-low voltage, the multiplying factor for the tariff is 0.5778cent. As assumed in the design part of solar dryer, the dryer works for 300days (because by considering holydays).

Therefore the cost required per year when we use electric is calculate as

=0.5778*26.48(KWhrs)*300=**4590**birr/year. (Saved cost by using solar dryer)

To calculate yearly cash flow, let as assume economic parameters:-

Interest rate (i) = 10%

Number of year (n) =6years.

Initial cost = 30855birr (cost of the dryer)

Operating cost (O) = 700birr (operating cost of the dryer)

Present cash flow (P) = 4590birr (the cost of electric energy saved by using solar dryer)

Future cash flow is given as:

$$F = P(1+i)^n \tag{9.1}$$

Table 8.3 Yearly Cash flow Analysis.

Year(n)	Interest rate(i)%	Operating cost at year n(ETB)	Future cost at year n(ETB)	Net Cash flow at year n(ETB)
1	10	770	5049	4279
2	10	847	5553.9	4706.9
3	10	932	6109.29	5177.29
4	10	1025	6720.219	5695.219
5	10	1127	7392.24	6265.24
6	10	1240	8131.46	6891.46

8.2.4 Payback Period

Determines the number of years required to recover an initial investment through project returns. Based on compound interest analysis as shown in the above table the payback period lasts given as follow. [25]

$$0 = -P + \sum_{t=1}^{t=pb} NCF_t (P/F, i, t) \tag{9.2}$$

Table 8.4 Cash Flow for Payback Period Analysis

End of year	0	1	2	3	4	5	6
Net Cash Flow(birr)	-30855	4279	4706.9	5177.3	5695.2	6265.2	6891.5
Cumulative Value(birr)	-30855	-26526	-21869.1	-16691.8	-10996.6	-4731.4	5160

From above table cumulative value at beginning of 6^{th} year is positive. Thus payback period is calculated from above table as; [25]

$$Pb = 5 + \frac{4731.4}{4731.4 + 5160} = 5.48 \text{years.}$$

CHAPTER NINE
Conclusion and Recommendation

Conclusion

Solar dryer for silica sand were simulated and tested. From experiment it were seen that solar dryer was best efficient in terms of drying rate, drying efficiency, moisture removal and variation of temperature through drying chamber than open sun drying technique. In solar dryer during rainy season it takes two day to dry 1kg of silica sand but in the sunny day it takes 1 day to dry the same quantity of silica sand but in open sun drying it takes three to four days. From this argument it was seen that, even if the weather condition was rainy (summer), silica sand was dried in solar dryer to meet demand, but in open sun drying method, it is difficult to dry silica sand during this weather condition. In addition to this open sun drying have its own draw back such as contamination with dusts materials and other impurities with silica sand were increased. The initial cost for solar dryer were high but once it was installed it has less operating cost and used for long period of time without any energy consumption or by using free available solar energy. To dry 178.4kg/day of silica sand, the required dimension solar dryer was designed.

Recommendation

To take the measurement of temperature through all drying beds or trays the number of sensors available was not enough. Because of this the reading were taken from selected number of trays. But to see all effects it was better to take the reading through all trays. Therefore for future work it better to conduct the experiment by adding the number of sensor to reading in all trays.

From the observation that were seen from the experiment, it was recommended that to use solar dryer to dry silica sand in order to maintain their productivity throughout the year even if its initial cost is high instead of using open sun drying technique.

Weather condition during this test was a little bit worst, for better result it was recommended to conduct the experiment in winter (sunny) season.

REFERENCE

1. Duffie J.A. and Beckman, W.A., Solar Engineering of Thermal Processes, Wiley, New York, 1991.
2. Potdukhe P. A. and Thombre S. B.: Development of a new type of solar dryer: Its mathematical modeling and experimental evaluation, Wiley Inter Science, 2008; 32:765–782.
3. Bolaji Bukola .O and. Olalusi Ayoola .P: Performance Evaluation of a Mixed-Mode Solar Dryer; Abeokuta, Ogun State, Nigeria; 2008.
4. Assefi Hossein and Atikol. U: Performance Potential of Flat Plate Solar Air Heaters in Tehran; Energy Research Centre; Eastern Mediterranean University; Famagusta via Mersin 10;Turkey;2009.
5. Ahmed Abed Gatea; Design, construction and performance evaluation of solar maize dryer; University of Baghdad, Iraq. March 2010; pp. 039-046.
6. Bolaji B.O., Analysis of Moisture Transport in the Solar Drying of Food Items; PMB 2240, Abeokuta, Nigeria.
7. Ashish kumar (80781005); Mathematical Modeling of Solar Air Heater with Different Geometries; A thesis submitted in partial fulfillment of the requirement for the award of degree of Master of Engineering in CAD/CAM & robotics; Thapar University Patiala-147004,July, 2009.
8. Mastekbayeva Gauhar A., Leon .M. Augustus and Kumar. S; Performance Evaluation of a Solar Tunnel Dryer for Chilli Drying; Energy Program, School of Environment, Resources and Development, Asian Institute of Technology.
9. Ion .V. Ion, Martins Jorge .G. Design, developing and testing of a solar air collector; University of Galati; Portugal ;2006.
10. Rajkumar Perumal; Comparative Performance of Solar Cabinet, Vacuum Assisted Solar and Open Sun Drying Methods; A thesis submitted to McGill University in partial fulfillment of the requirements for the degree of Master of Science; Canada, February, 2007.

11. Alfegi Ebrahim M. Ali, Sopian Kamaruzzaman, Othman Mohd Yusof Hj and Yatim Baharudin Bin; Mathematical Model of Double Pass Photovoltaic Thermal Air Collector with Fins; University Kebangsaan Malaysia; 2009, 592-598.
12. Simate I.N. Optimization of Mixed-Mode and Indirect-Mode Natural Convection Solar Dryers; Lusaka, Zambia, March 2002, 435–453.
13. Forson .F.K. , Nazha M.A.A., Akuffo F.O. and Rajakaruna H. Design of mixed-mode natural convection solar crop dryers: Application of principles and rules of thumb; Kumasi, Ghana, (2007) 2306–2319
14. Luna .D, Nadeau .J.Pand Jannot. Y; Model and simulation of a solar kiln with energy storage; France, 2010, 2533-2542.
15. Ekechukwu. O.V. , Norton. B; Review of solar-energy drying systems II: an overview of solar drying technology Northern Ireland, U.K, 1999, 615-655.
16. Weiss. Werner and Buchinger.Josef; Establishment of a Production, Sales and Consulting Infrastructure for Thermal Plants. Zimbabwe Institute for sustainable Technologies A-8200 Gleisdorf, Feldgasse, 19 Austria.
17. Habtamu Tkubet Ebuy; Simulation of Solar Cereal Dryer Using Transys; A thesis submitted to the School of Graduate Studies of Addis Ababa University in partial fulfillment of the requirements for the Degree of Masters of Science in Mechanical Engineering, Addis Ababa, Ethiopia,2007.
18. Gupta. M.K. and Kaushik .S.C; Exergetic performance evaluation and parametric studies of solar air heater; Indian Institute of Technology, Delhi 110016, India, 2008.
19. Misrak Girma; Performance Analysis of Solar Power Still. A thesis submitted to the School of Graduate Studies of Addis Ababa University in partial fulfillment of the requirements for the Degree of Masters of Science in Mechanical Engineering, Addis Ababa, Ethiopia, 2009.
20. Kituu G. M., Shitanda D., Kanali C. L, Mailutha J. T, Njoroge C. K, Wainaina J. K, Bongyereire J. S, Simulation model for solar energy harnessing by the solar tunnel dryer; Nairobi, Kenya;2010.
21. Janjai .S, Tung .P; Performance of a solar dryer using hot air from roof-integrated solar collectors for drying herbs and spices, Thailand, 2005.

22. FOLARANMI Joshua; Design, Construction and Testing of Simple Solar Maize Dryer, Niger State, Nigeria, July-December 2008, p. 122-130.
23. Aklilu Tesfamichael; Experimental Analysis for Performance Evaluation of Solar Dryer, Addis Ababa University School of Graduate studies Department of Mechanical Engineering.
24. http://www.LabVIEWtutorial.com.net
25. http://www.paybackperiodanalysis.com.net

Appendix A

Results Observed During Test

Table A-1 Shows Daily Data Recorded During Experiment.

No	Days of test conducted	Trays	Mass of water removed (gm)	Moisture content (wet basis)	Drying rate(gm/sec)	Efficiency (%)
1	May 23	1	226	0.18	0.89	14.08
		2	189	0.15	0.75	11.8
		3	100	0.08	0.4	6
2	May 24	1	125	0.1	0.5	7
		2	106	0.084	0.42	6.6
		3	97	0.08	0.38	6.04
3	May 25	1	348	0.25	1.38	21.7
		2	154	0.1	0.611	10
		3	66	0.051	0.26	4.01
4	June 20	1	186	0.186	0.74	13.2
		2	184	0.184	0.73	13.04
		3	168	0.168	0.67	11.91
		4	141	0.141	0.56	10
		5	140	0.140	0.55	9.9
5	June 21	1	78.5	0.091	0.311	5.61.13
		2	60	0.07	0.24	4.3
		3	57	0.069	0.23	4.04
		4	54	0.066	0.214	2.83
		5	16	0.02	0.0635	1.13
6	open sun drying (May25)		154	0.11	0.611	

Appendix B

Figure B-1 Shows Mass Balance of Silica Sand during Experiment.

Figure B-2 Temperature Reading on Lab View Experimentally

Figure B-3 Sensor Positioning to Take Reading Experimentally

Figure B-4 Experimental Investigation of Moisture Content